AD NUMBER
AD042960

CLASSIFICATION CHANGES	
TO:	unclassified
FROM:	confidential

LIMITATION CHANGES

TO:

Approved for public release; distribution is unlimited.

FROM:

Distribution authorized to DoD only; Administrative/Operational Use; MAY 1954. Other requests shall be referred to Office of Naval Research, One Liberty Center, Suite 1425, 875 North Randolph Street, Arlington, VA 22203-1995. Pre-dates formal DoD distribution statements. Treat as DoD only.

AUTHORITY

31 May 1966, DoDD 5200.10; ONR ltr dtd 9 Nov 1977

UNCLASSIFIED

AD _____

Reproduced
by the

ARMED SERVICES TECHNICAL INFORMATION AGENCY
ARLINGTON HALL STATION
ARLINGTON 12, VIRGINIA

CONFIDENTIAL

FCL 7203-T-16

DESIGN AND TEST OF A LONGITUDINAL CONTROL SYSTEM FOR A HYDROFOIL CRAFT

by

Brian T. Hastings

Francis W. Penney

James B. Baker

May 1954

FLIGHT CONTROL LABORATORY
MASSACHUSETTS INSTITUTE OF TECHNOLOGY

CAMBRIDGE 39, MASS.

OCT 21 1954

CONFIDENTIAL 54AA 65996

DESIGN AND TEST OF A LONGITUDINAL CONTROL SYSTEM
FOR A HYDROFOIL CRAFT

by

Brian Tuite Hastings, Capt., USAF
B.A.E. New York University, 1949

Francis Wood Penney, 1st Lieut., USAF
B.S.M.E. University of New Hampshire, 1951

James Burnell Baker, 1st Lieut., USAF
B.E.E. North Carolina State College, 1952

SUBMITTED IN PARTIAL FULFILLMENT OF THE
REQUIREMENTS FOR THE DEGREE OF
MASTER OF SCIENCE

at the

MASSACHUSETTS INSTITUTE OF TECHNOLOGY
1954

Signature of Authors _Brian T. Hastings_

Francis W. Penney

James B Baker

Dept. of Aeronautical Engineering, May 24, 1954

Certified by _Robert C. Seamans Jr_

Thesis Supervisor

Shatswell Ober.

Chairman, Departmental Committee on Graduate Students

1

This thesis, written by the author while assigned to Massachusetts Institute of Technology, has been reproduced by the offset process using printer's ink in accordance with the following basic authorization received by Dr. C. S. Draper, Director of the Instrumentation Laboratory.

COPY

April 7, 1950

Dr. C. S. Draper
33-103

Dear Dr. Draper:

Mr. L. E. Payne has shown to me a recent printed reproduction of a thesis, in this instance a Master's dissertation, submitted in partial fulfillment of the requirements for the degree of Master of Science at the Massachusetts Institute of Technology.

The sample shown is printed by the offset press using screened illustrations, graphs and other material. For the purposes of the Library which include record and permanent preservation, theses reproduced in this manner are perfectly satisfactory and in my opinion meet all of the physical requirements of the graduate school insofar as they pertain to the preparation of a thesis.

I note that in the sample submitted the signatures have been reproduced along with the text by photo lithography. It is suggested that for the Library record copy the author, thesis supervisor and chairman of the Departmental Committee on Graduate Students affix their signatures in writing as complete authorization of the study. These can be written above the reproduced signature if desired.

Sincerely yours,

(signed)

Vernon D. Tate
Director of Libraries

VDT/ji

cc: Dean Bunker
Mr. Payne

COPY

2

DESIGN AND TEST OF A LONGITUDINAL CONTROL SYSTEM
FOR A HYDROFOIL CRAFT

by

Brian Tuite Hastings
Francis Wood Penney
James Burnell Baker

Submitted to the Department of Aeronautical Engineering on
May 24, 1954, in partial fulfillment of the requirements for the
degree of Master of Science.

ABSTRACT

A hydrofoil craft, when under way, can be described as a hull
supported clear of the water by the dynamic lift of underwater wings
or hydrofoils. Such craft have decided advantages in speed per horse-
power and in seakeeping ability. The serious problem involved is to
stabilize the craft against disturbances due to water surface and sub-
surface motion.

This thesis proposes a guidance and control system which includes
an integrating gyro for craft pitch control, a device for sensing posi-
tion of the water surface, and a device for measuring water motion
beneath the surface. The craft and control system are then tested for
response to sinusoidal waves.

The equations of motion for the craft are presented and certain
simplifying assumptions made. Various relating functions for the
craft are developed and gain-phase diagrams plotted. From the
diagrams are calculated the loop gains sufficient to cause conditional
stability of the system. This gain is then used as an accuracy check
against the gain which causes conditional stability of the electronically
simulated system.

Simulator test results show that more control is lost than gained
through use of the sub-surface water sensing device. It is therefore

discarded. The authors believe that the guidance and control system as thus reduced will give substantially better performance than any system which has been tried on the craft studied. Suggestions are offered for further improvement.

Thesis Supervisor: Robert C. Seamans, Jr.
Title: Associate Professor of
                Aeronautical Engineering

May 24, 1954

Professor Leicester F. Hamilton
Secretary of the Faculty
Massachusetts Institute of Technology
Cambridge 39, Massachusetts

Dear Professor Hamilton:

In accordance with the regulations of the faculty, we hereby

submit a thesis entitled Design and Test of a Longitudinal Control

System for a Hydrofoil Craft in partial fulfillment of the require-

ments for the degree of Master of Science.

Brian T. Hastings
Brian Tuite Hastings

Francis W. Penney
Francis Wood Penney

James B. Baker
James Burnell Baker

ACKNOWLEDGMENTS

The authors express their appreciation to the personnel of the Flight Control Laboratory of the Massachusetts Institute of Technology who assisted in the preparation of this thesis. Particular thanks are due to Professor Robert C. Seamans, Jr., for his guidance and enthusiasm. Messrs. Frank Barnes, Joseph Connors, and David Wellinger were very generous of their time and of their knowledge of the hydrofoil; and Mr. Roger Phagan answered many questions in our introduction to and use of the Flight Control Laboratory analogue computer.

The graduate work for which this thesis is a partial requirement was performed while the authors were assigned by the Air Force Institute of Technology for graduate training at the Massachusetts Institute of Technology. The thesis was prepared under the auspices of D.I.C. Project 7203 sponsored by Office of Naval Research through Contract NONR-507(00). The hydrofoil craft which is the subject of this thesis was designed by Gibbs and Cox, Inc., Naval Architects and Marine Engineers, of New York.

CONFIDENTIAL

TABLE OF CONTENTS

CONFIDENTIAL

LIST OF ILLUSTRATIONS

LIST OF TABLES

OBJECT

The object of this thesis is to design and test, with an electronic simulator, a longitudinal guidance and control system for a hydrofoil craft. The problem is similar to the design of a pitch-attitude automatic pilot for an airborne vehicle, with the additional difficulty that the hydrofoil is subject to continual large scale water disturbances, and with an additional requirement for precise control of altitude to within a few inches.

CHAPTER 1

INTRODUCTION

1.1 Nature of the Problem

A hydrofoil craft may be described as a hull supported clear of the water, when under way, by the dynamic lift of underwater wings, or hydrofoils.[2] For certain speed-length ratios it offers a substantial reduction in water resistance, a corresponding increase in speed per horsepower, and a marked improvement in sea keeping ability. Various craft and foil configurations are possible, but for craft larger than twenty-five to fifty tons, the most promising system seems to have two or three controllable and fully submerged foils.[2] (See Fig. 1.1.)

Various investigators have experimented with hydrofoil craft since about the turn of the century. Among the well-known inventors and scientists may be found such names as Wilbur and Orville Wright, Alexander Graham Bell, and Otto Tietjens. Results have varied from poor to very good, but the good results have been accomplished only in relatively smooth water. One of the reasons for the lack of success has been that the problems of hydrofoil flight are inherently more complicated than those of subsonic aerodynamics; and there has not been so much study made of the hydrofoil as of the airplane.

The chief problem in hydrofoil design has been, and is now, stabilization of the craft in a seaway. Recent controlled-foil systems have been successful in so-called head seas, but the problem of the following sea remains. (See Appendix A.)

A good control system will probably be similar in general nature to an aircraft automatic pilot.[15] However, it must in addition provide precise control of altitude within a few inches, and it must be able to handle continuous and large scale disturbing inputs.
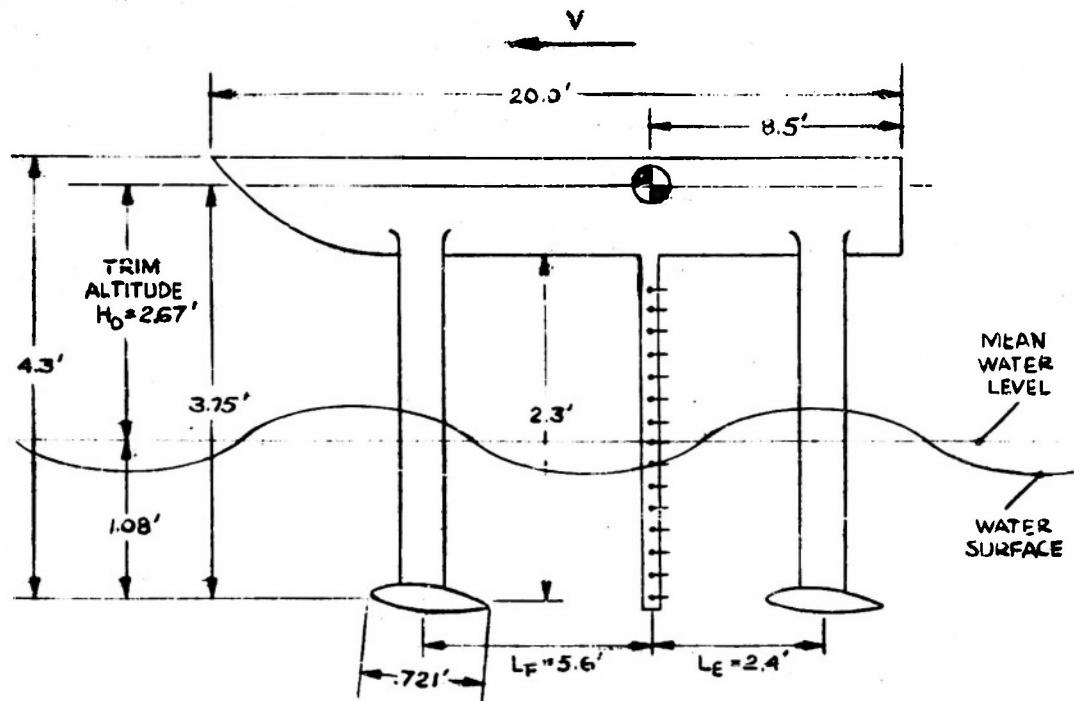
FIG. 1-1 SKETCH OF HYDROFOIL CRAFT.

1.2 Current Research Efforts

The dimensions shown in Fig. 1.1 are for the small research craft
designed under U.S. Navy auspices by the Gibbs and Cox Corporation.
It is hoped that the study of this small craft will produce fundamental
knowledge of hydrofoil performance which will be useful in the design
of larger craft.   The Flight Control Laboratory of Massachusetts Insti-
tute of Technology is undertaking a fundamental and general study of
submerged-foil hydrofoil craft.   The object of this thesis, based on
present development of the Flight Control Laboratory study, is narrower
and more specific.   The object of this thesis is to design a longitudinal
control system for the present Gibbs and Cox craft.   Because of limited
time the study has been confined to minor variations of one basic con-
trol system, and sea conditions have been specified as sinusoidal steady-
state.   The craft and the water have been simulated and tested on the
Flight Control Laboratory Electronic Analogue Computer.

CHAPTER 2

PROPOSED LONGITUDINAL GUIDANCE AND CONTROL SYSTEM

2.1 General description of system

The hydrofoil craft in flight is subject to two disturbances. The first arises from the fact that the craft must rely for guidance on some measure of the water level – but the water surface is continually moving up and down to disturb the craft. The second arises from the sub-surface orbital motion described in Appendix A and from the consequent continual changes in the lift and drag forces generated by the hydrofoil surface.

This thesis attempts to solve these problems. Figure 2-1 is a sketch of the craft being studied, with definitions of the quantities involved. Figure 2-2 is a block diagram of the guidance and control system proposed. As described below, the pitch and altitude control systems will attempt to minimize deviations from a reference pitch angle and a reference altitude. The guidance system will attempt to guide the craft up and over larger waves. The combined system can be said to have three objectives:

1. Maintain a nearly constant altitude with the rear foil as follows. Install at the rear foil a device, hereafter called a water vane, which will swing about a hinge so that it is continuously lined up with the water velocity direction. Through an electrical resolver, develop a signal which will slave the servo-controlled rear foil at a normal, or trim angle to the water vane. Under control of a height sensing device at the center of gravity, change the angle between vane and foil (which is the effective foil angle of attack) as necessary to provide more or less lift.

2. Maintain a nearly constant craft pitch angle with the front foil as follows. Install a very fast integrating gyro which will sense any angular deviation of the craft in pitch from a reference direction and send a correcting signal to the front foil servo.

3. In high seas, command changes in craft pitch angle and height to follow the slope of the waves. Develop pitch commands by installing a
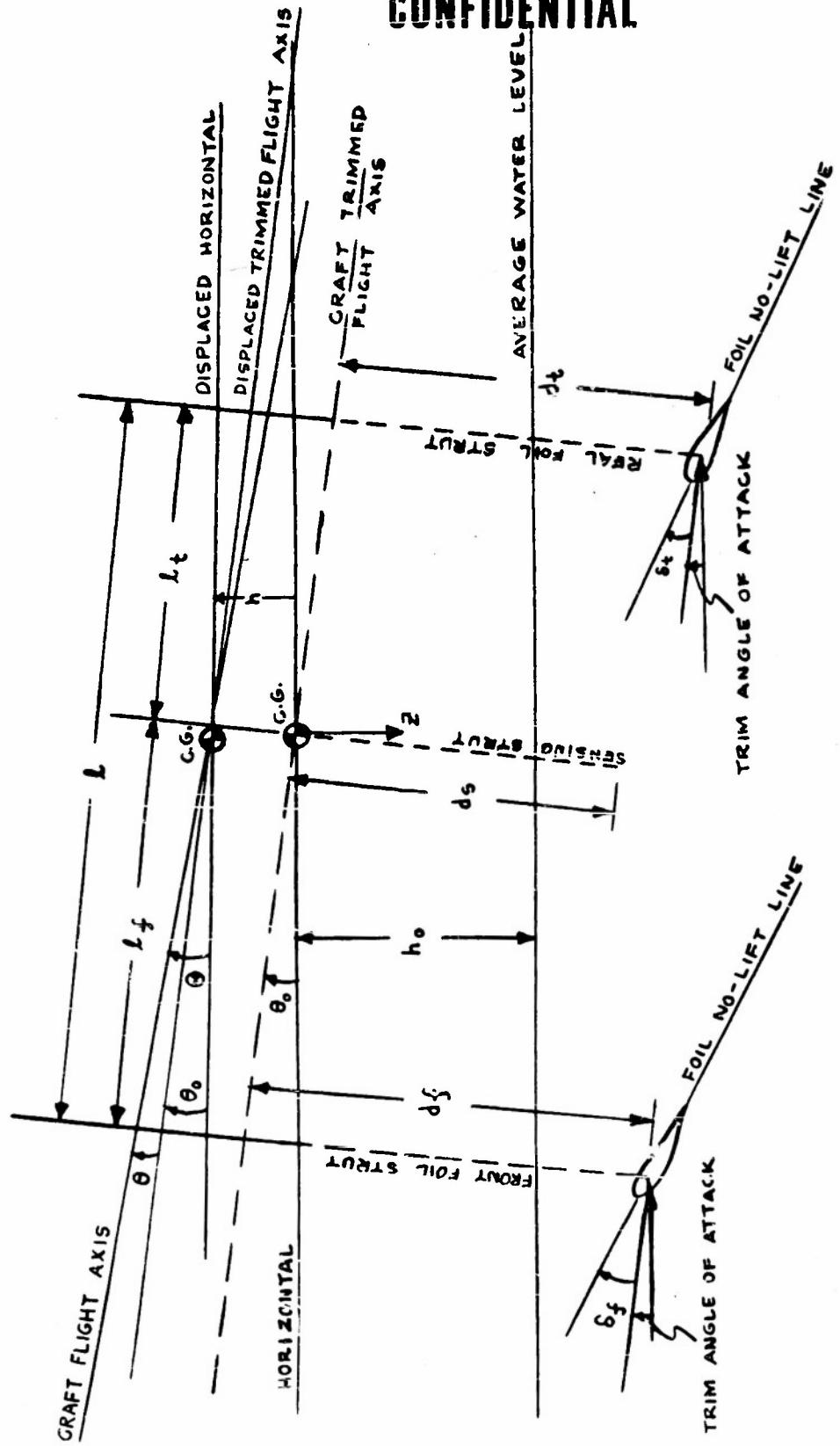
FIG. 2-1 HYDROFOIL CRAFT IN FLIGHT
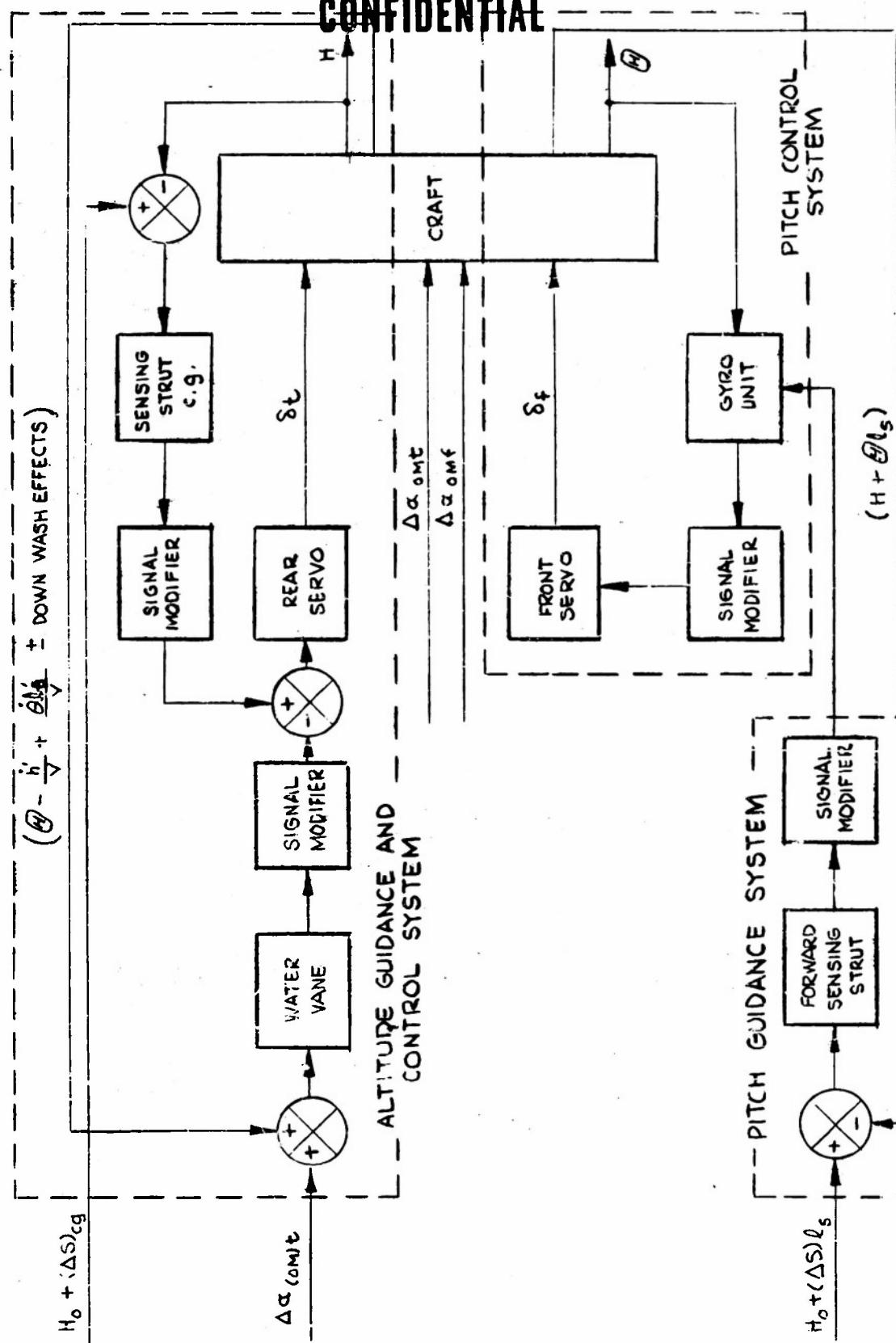
FIG 2·2 BLOCK DIAGRAM OF PROPOSED LONGITUDINAL GUIDANCE AND CONTROL SYSTEM

second, and different, height sensing device forward of the bow of the boat; this device will send commands to the torque generator in the gyro unit to establish new reference pitch angles as necessary. Develop height commands at the height sensing device which is at the center of gravity.

2.2 Height-sensing strut at center of gravity

The height-sensing strut installed in the present Gibbs and Cox craft is sketched below.
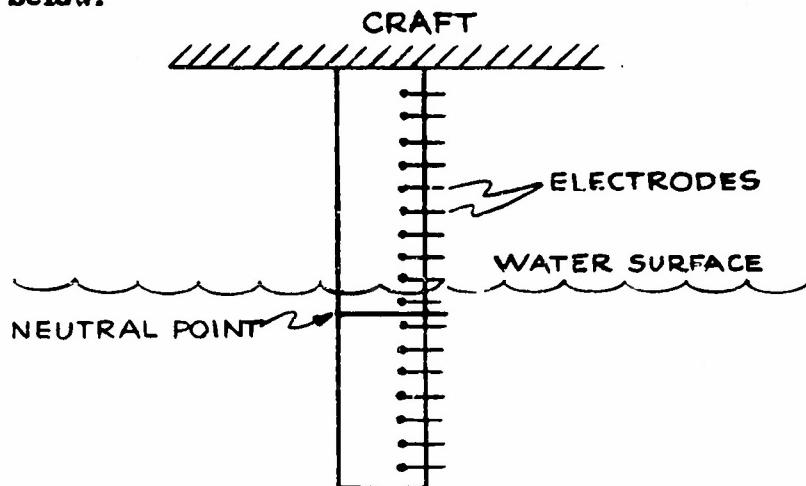
When an electrode is immersed in the water it is grounded to the strut and craft. The number of grounded electrodes is a measure of the depth of the strut or the height of the craft. The signals from the electrodes are of opposite polarity above and below the neutral point to establish craft reference height. If water is higher on the strut than the neutral point, the strut signal is a command for the craft to climb, and conversely. This thesis has assumed that there is a negligible delay between water clearance time and drying time of an electrode. It is also assumed that the electrodes are spaced closely enough that the signal can be considered continuous rather than discrete.

2.3 Height-sensing strut forward of the bow

The forward sensing strut is mounted ahead of the bow of the boat to guide the craft up and down the slopes of larger waves by sending a signal to the gyro torque generator or directly to the front foil, or to both. Its

principle of operation is similar to the sensing strut at the center of gravity. However, it is desired that the craft fly straight and level through smaller waves and follow only the larger waves. Therefore the forward strut has a dead zone in which smaller waves may move up and down to produce either a small signal or no signal at all. The width of the dead zone and the magnitude of the two zone signals are to be determined by analysis or experiment with due consideration for the problem of gyro drift.

2.4 The servo motor

The motors controlling the front and rear servos are conventional but high performance electrical positional servos. The authors have assumed availability of a servo with a natural frequency of 30 radians per second (4.78 cycles per second) and a damping ratio of 0.7.

2.5 The Integrating Gyro

The integrating gyro is a single-degree-of-freedom, or single-gimbal, gyroscope. It receives as its input the angular velocity of its case about the input axis, with respect to inertial space, along with electrical current input signals to its torque generator, and generates an output voltage proportional to the time integral of these inputs.[14] The gimbal housing is completely immersed in a damping fluid which provides an opposing shear force proportional to gimbal angular rate. The result is that the angle of the gimbal with respect to the case at every instant of time is proportional to the angular displacement of the case about the input axis measured with respect to inertial space.

The operation of the Type H Integrating Gyro is described in detail in Reference 14. For the purpose of this thesis the integrating gyro can be considered as a fast, precise device with three characteristics:

1. The gyro will provide an electrical signal proportional to the pitch angle by which the hydrofoil craft longitudinal axis has rotated from a reference direction.

2. The gyro will accept an electrical signal as a command to change the reference direction in inertial space.

3. The gyro is very fast. A typical characteristic time, or time constant, is 0.00285 sec. This is so much faster than hydrofoil craft response times that gyro dynamics can and will be ignored.

17

2.6   The water vane

A major factor in hydrofoil performance is the water orbital motion and its effect on the local water velocity direction at the foil. Various methods of continuously measuring this direction suggest themselves. Several methods will be mentioned briefly in Chapter 5 on Suggestions. A fairly simple and seemingly feasible method has been assumed for this thesis. It is based on the venerable concept of the weather vane. The actual design and fabrication of the device will be a project in itself but in this thesis the authors have assumed that the device can be built and that its dynamics will be negligible.

The water vane will probably be based on a symmetrical airfoil or hydrofoil section, hinged near or ahead of its leading edge and flying freely in the water flow. Its configuration and location will depend among other things on considerations of water flow and vortex patterns. The authors do not believe that the device must accurately measure foil angle of attack, with all the attendant problems that are known to exist in the design of aircraft angle of attack indicators. It seems sufficient that the water vane indicate a reasonably accurate reference direction. For example if it is necessary to locate the vane in or near a foil tip vortex, or in the downwash, it is only necessary that the vane angle bear some simple and reasonably accurate relation to the actual direction of water flow. Note that the vane will automatically allow for downwash at the rear foil due to the front foil.

From the hinge the vane orientation can be transmitted to an electrical resolver by means of a simple wire and pulley system; the wires might be carried up the inside of the structure which connects the hull with the foil. Or the resolver might be mounted in a water proof housing at the foil with the electrical signal transmitted to the hull. Resolvers are commercially available which will measure angles as small as 0.002 radian. The electrical signal from the resolver can then be added to the signal from the height-sensing strut and used as the error signal to the positional servo controlling the foil.

Note that in trim flight in smooth water the servo will not be commanded to line up the foil with the vane; it will be commanded to establish a trim angle of attack between foil and vane. When the craft encounters

orbital motion the resolver signal will command a change in foil angle with respect to a reference in the craft, without any change in the angle between foil and vane. When the craft encounters a wave or a change in height the strut signal will also command a change in the angle between foil and craft, but this change will amount to a change in angle between foil and vane.

This thesis is concerned only with longitudinal control of the craft but a brief consideration of the lateral control problem suggest two alternatives. The first is to mount only one water vane between the two rear foils and use it as a reference for both. The second is to mount two water vanes, one outboard of each of the two rear foils. The latter might prove more effective in the problem of lateral control where it will be important to consider the variation of water velocity direction from one side of the craft to the other. Again the designer will have to make a reasonable compromise and consider vortex and downward effects.

CHAPTER 3

SYSTEM ANALYSIS AND TEST PROCEDURE

3.1 Simulation of System

The guidance and control system proposed in Fig. 2-2 was simulated on the Flight Control Laboratory Electronic Analog Computer. This computer is a real time computer similar to the better known Reeves Analog Computer. The simulated system is shown in Appendix E, Fig. E-1. The system was analyzed using an expanded time scale (i.e., one second real time equals ten seconds computer time) because of the dynamic range of gains involved.

Some organized method for selecting loop gains had to be used. The authors chose to select each guidance and control loop gain on the basis of system responses to individual disturbance inputs. The pitch control system loop gain was set first, because the altitude control system (Eq. (C-14)) is unstable without the pitch control system operating.

3.2 Pitch Control System

The purpose of the pitch control system is to minimize craft pitch rate caused by disturbing inputs. The integrating gyro measures pitch rate and provides a correcting signal to the front foil.

The pitch control system includes a signal modifier which was not described in Chapter 2. After several design considerations, the only logical choice for this signal modifier seemed to be a lead-lag network (Eq. (D-2)). It is normally desired that the characteristic time ratio (α) be as large as possible and is set equal to 10 because this is close to the practical design limit for such a network. Three values of the characteristic time (τ_{SM}) were chosen as .01, .02, and .03 seconds. With these values, gain-phase diagrams similar to Fig. D-1 were drawn. From these diagrams, the design characteristic time was

chosen as .01 second, because this value gives a gain margin[16] of 7.1, approximately 150% and 300% of that for .02 and .03 respectively. The phase margin was approximately 60 degrees for all characteristic time values used; therefore, gain margin alone was used to select the characteristic time of the signal modifier.

Now all the features of the pitch control system have been specified except the feedback sensitivity. Disturbance inputs in the form of variable frequency sinusoidal waves representing orbital motion at the front foil were used to select this gain. All the sea conditions of Appendix A, Fig. A-3 were simulated, and the best value of the feedback sensitivity ($S_{gu} S_{FS}$, foil deflection per unit pitch angle) was found to be between −2 and −4 from consideration of the magnitude of the front foil deflection and craft pitch angle. A higher sensitivity would further reduce the pitch angle, but this would cause larger foil deflections and might stall the foil. Therefore, the maximum sensitivity investigated was −4.

3.3 Altitude Guidance and Control System

The altitude guidance and control system has to be studied with the pitch control system operating since the altitude system alone is unstable. The feedback sensitivity of the pitch control system was set at −2 for this study.

All components of the altitude control system (omitting the water vane loop) were specified in Chapter 2 except the signal modifier. Because of simulator equipment limitations, the only network that could be tried was a filter network. This network introduced additional lags in the system and was undesirable. It was therefore omitted. The best network would seem to be a lag-lead network giving approximate integral control, but the lack of additional components on the computer canceled this study.

For disturbance inputs representing orbital motion at the rear foil, the best value of altitude feedback sensitivity ($S_{SE} S_{RS}$, foil deflection per foot change in height) was between −0.3 and −0.6 for the purpose of minimizing deviations in the height of the craft. However, when the single input was used to represent the sea surface, these values of

feedback sensitivity were found to be too large at the higher frequencies because of system lags. The best value of feedback sensitivity at these higher frequencies was found to be between $-.015$ and $-.030$.

Thus one sees that a rough sea puts contradicting requirements on the altitude guidance and control system – high feedback sensitivity to combat orbital motion and low sensitivity to minimize sea surface effects. One approach to handling this double requirement is to combat orbital motion by another control system loop. The water vane control loop (Fig. 2-2) was proposed. As before, computer components limited the equipment in this system, and the signal modifier was reduced to a pure sensitivity (S_{WV}). With the altitude control system feedback sensitivity ($S_{SE} S_{RS}$) equal to $-.02$ rad/foot and a single disturbance input representing orbital motion at the rear foil, the best value of the water vane control system gain ($S_{WV} S_{RS}$, radian per radian) was between 1 and 2 depending upon the sea condition (frequency).

On the basis of single inputs, the ranges of the control system gains have been specified. Now, the entire control is ready to be tested using multiple inputs (Appendix A). However, the proposed method for developing a pitch rate to ride long-wavelength, high-amplitude waves has not been discussed.

3.4 Pitch Guidance System

The proposed method for developing a pitch rate to ride long-wavelength, high-amplitude waves is shown in Fig. 2-2. This system was not simulated on the computer for the same reason mentioned several times previously – lack of computer equipment.

The proposed sensing element for the system is discussed in Section 2.3. Its output signal can be used for guidance in several ways. One method is to use the signal to torque the integrating gyro, calling for a pitch rate proportional to the signal. Another method consists of two steps: (1) use the dead-zone, low-amplitude signal to torque the gyro as a correction for gyro drift, and (2) use the outer-zone, high-amplitude signal as an input to the signal modifier calling for a craft pitch rate to null the signal through gyro feedback. This entire guidance system needs further study before a definite arrangement of equipment can be specified.

3.5 Guidance and Control System Test

Multiple inputs (Appendix A) representing orbital motion at the front and rear foils and sea surface at the center of gravity of the craft were used to test the guidance and control systems described in Sections 3.2 and 3.3. The first multiple input used for test was a 40-foot wavelength following sea using these sensitivities: $S_{gu} S_{FS} = -2.0$, $S_{SE} S_{RS} = -.020$, and $S_{WV} S_{RS} = 1.0$. The result was that both front and rear foils broached. Several combinations of sensitivities were tried with the water vane system included and then omitted completely, and the final conclusion was that the water vane system did more harm than good. (Refer to Chapter 5 for explanation.) Time limitations forced the authors to remove the water vane from the system without further exploration of its possibilities. Further study is recommended for future investigators to determine the potentialities of a water vane.

With the omission of the water vane control system, the rest of guidance and control system was tested. The sea conditions chosen were head and following seas of 10, 20, and 40 foot wavelengths. The responses of the hydrofoil craft to these sea conditions for various combinations of system feedback sensitivities were recorded on a Sanborn recorder and are tabulated in Table 3-1. All values tabulated are the maximum values of the variable [i.e., $q = q_{max} \sin (wt + PA)$]. The phase angles of the craft height deviation with respect to the water surface $(\Delta S - h)$, craft height deviation with respect to inertial space (h), the pitch angle deviation (θ), and the sea surface at the front and rear foils are measured with respect to the sea surface at the center of gravity of the craft and tabulated as $PA_{[\Delta S; (\Delta S - h)]}$, $PA_{[\Delta S; h]}$, $PA_{[\Delta S; \theta]}$, $PA_{[\Delta S; \Delta S_f]}$ and $PA_{[\Delta S; \Delta S_t]}$ respectively.

From the data of Table 3-1, one can calculate the depth of submergence of the rear and front foils. The necessary equations are:

$$\text{depth of submergence of front foil} = \text{Trim submergence} + (\Delta S)_{max} \sin [wt + PA_{[\Delta S; \Delta S_f]}]$$

$$- \ell_f \theta_{max} \sin (wt + PA_{[\Delta S; \theta]})$$

$$- h_{max} \sin [wt + PA_{[\Delta S; h]}]$$

TABLE 3-1

SUMMARY OF COMPUTER RESULTS

Wave length (ft)	Wave Double Amplitude (ft)	Frequency (cps)	$B_{BM} g_{BM} g_{PE}$ (rad/rad)	$g_{BE} g_{PE}$ (rad/rad)	$(\Delta\sigma_{OM})_{max}$ (rad)	$(\Delta\beta)_{max}$ (ft)	h_{max} (ft)	$(\Delta\beta-h)_{max}$ (ft)	β_{max} (rad)	$\theta_{1(max)}$ (rad)	$\theta_{1(max)}$ (rad)	$PA_{[\Delta\beta;(\Delta\beta-h)]}$ (deg)	$PA_{[\Delta\beta;\theta]}$ (deg)	$PA_{[\Delta\beta;h]}$ (deg)	$PA_{[\Delta\beta;\Delta\beta_7]}$ (deg)	$PA_{[\Delta\beta;\Delta\beta_7]}$ (deg)
HEAD SEA																
10	0.5	3.72	2.0	0.02	0.020	0.250	0.010	0.28	0.001	0.004	0.004	350	75	350	202	86
10	1	3.72	2.0	0.02	0.040	0.500	0.020	0.52	0.002	0.008	0.008	350	75	350	202	86
20	1	2.05	2.0	0.02	0.039	0.500	0.028	0.10	0.015	0.050	0.010	0	42	249	101	43
20	1	2.05	2.0	0.30	0.039	0.500	0.300	0.73	0.053	-	-	0	43	194	101	43
20	2	2.05	2.0	0.02	0.078	1.000	0.052	1.00	0.030	0.100	0.020	0	14	249	101	43
20	2	2.05	2.0	0.30	0.078	1.000	0.600	1.58	0.106	-	-	0	43	194	101	43
40	2	1.11	2	0.30	0.064	1.000	1.15	0.97	0.172	0.437	0.301	82	139	311	50.5	21.5
40	2	1.11	2	0.60	0.064	1.000	1.25	0.56	0.178	0.453	0.347	98	198	344	50.5	21.5
40	2	1.11	4	0.30	0.064	1.000	1.44	1.18	0.125	0.810	0.387	84	196	311	50.5	21.5
40	2	1.11	4	0.60	0.064	1.000	Unstable									
FOLLOWING SEA																
10	0.5	2.29	2.0	0.02	0.020	0.25	0.018	0.24	0.003	0.011	0.004	298	244	42	202	86
10	1	2.29	2.0	0.02	0.040	0.50	0.035	0.47	0.008	0.022	0.008	298	244	42	202	86
20	1	1.00	2.0	0.02	0.039	0.50	0.148	0.64	0.033	0.081	0.053	355	321	156	101	43
20	1	1.00	2.0	0.30	0.039	0.50	0.515	0.61	0.056	0.145	0.193	63	136	290	101	43
20	1	1.00	2.0	0.60	0.039	0.50	0.596	0.35	0.076	0.217	0.210	92	180	327	101	43
20	1	1.00	4.0	0.30	0.039	0.50	0.645	0.89	0.036	0.193	0.210	70	187	290	101	43
20	2	1.00	4.0	0.60	0.039	0.50	Unstable									
20	2	1.00	2.0	0.02	0.078	1.00	0.29	1.28	0.066	0.164	0.103	355	321	156	101	43
20	2	1.00	2.0	0.30	0.078	1.00	1.03	1.22	0.112	0.290	0.386	63	136	290	101	43
20	2	1.00	2.0	0.60	0.078	1.00	1.19	0.70	0.152	0.434	0.420	92	180	327	101	43
20	2	1.00	4.0	0.30	0.078	1.00	1.29	1.38	0.078	0.386	0.420	70	187	290	101	43
20	2	1.00	4.0	0.60	0.078	1.00	Unstable									
40	2	0.392	2.0	0.30	0.064	1.00	0.97	0.79	0.117	0.242	0.242	57	237	317	50.5	21.5
40	2	0.392	2.0	0.60	0.064	1.00	1.03	0.56	0.140	0.287	0.250	90	246	334	50.5	21.5
40	2	0.392	4.0	0.30	0.064	1.00	1.06	0.56	0.041	0.183	0.182	90	270	334	50.5	21.5
40	2	0.392	4.0	0.60	0.064	1.00	Unstable									
40	2	0.392	1.5	0.25	0.064	1.00	0.787	0.91	0.121	-	-	43	187	301	50.5	21.5
40	2	0.392	1.5	0.50	0.064	1.00	0.650	0.48	0.152	-	-	49	194	317	50.5	21.5
40	2	0.392	1.5	0.75	0.044	1.00	0.911	0.42	0.151	-	-	66	214	340	50.5	21.5
40	2	0.392	3.0	0.25	0.064	1.00	1.06	0.82	0.066	-	-	74	248	317	50.5	21.5
40	2	0.392	3.0	0.50	0.064	1.00	0.545	0.43	0.079	-	-	83	248	340	50.5	21.5
40	2	0.392	3.0	0.75	0.064	1.00	Unstable									
40	2	0.392	4.5	0.25	0.064	1.00	0.530	0.096	0.030	-	-	74	243	320	50.5	21.5
40	2	0.392	4.5	0.50	0.064	1.00	0.545	0.364	0.045	-	-	77	266	343	50.5	21.5
40	2	0.392	4.5	0.75	0.064	1.00	Unstable									

depth of submergence
of rear foil

$$= \text{Trim submergence} + (\Delta S)_{max} \sin[wt - PA_{[\Delta S; \Delta S_t]}]$$

$$+ \mathring{\ell}_t \theta_{max} \sin[wt + PA_{[\Delta S; \theta]}]$$

$$- h_{max} \sin[wt + PA_{[\Delta S; h]}]$$

A check of the data shows that both foils are at least under the water
surface for some combination of sensitivities at all sea conditions in-
vestigated. However, the foils are not always submerged as much as
nine-tenths of the foil chord. Therefore, the assumption about the
height derivatives in the derivation of the equations of motion (Ap-
pendix B) has been violated. The addition of the height derivatives
would seem to help keep the foils submerged since their major effect
is a decrease in effective lift as the foil approaches the surface. This
decrease in lift may be enough to keep the foils submerged the required
depth. However, this is something that must be discovered by further
investigation.

CHAPTER 4

CONCLUSIONS

4.1 General

The general conclusion from the test results of Table 3-1 is that the proposed guidance and control system gives better craft performance than any system which has been installed and tested on the same configuration of the Gibbs and Cox craft. The proposed system also gives better performance than earlier systems studied by the Flight Control Laboratory. The reasons for the improvement lie in the use of the integrating gyro and the addition of a rear foil servo, two components which have not been investigated very thoroughly before. Further, the servo used in this thesis is assumed to have better performance than those actually installed in the research craft.

The sea conditions simulated are a reasonable representation of a variety of undisturbed waves. Test results show that for each sea condition tested there is at least one combination of system gains which keeps the front and rear foils submerged; note, however, that in most cases the foils do come closer to the surface than nine-tenths of a chord length. In the derivation of the craft equations of motion it was assumed that the foils would stay below the surface by at least this distance. This made it possible to linearize certain relationships and neglect height derivatives. The nonlinearities arise from the fact that the foil loses lift very rapidly as it rises above this critical depth. Now if test results show the foil to be rising higher than this critical depth it is indeed true that the mathematical representation of the craft is no longer valid. However, as the foils make their close approach to the surface, the loss of lift probably prevents the craft from rising as far as the mathematical model indicates. Therefore, the authors believe that in every sea condition tested the foils did in fact remain at a safe depth.

The general results stated above depend on changing the gain in both loops as a function of sea condition. The <u>pitch</u> <u>control</u> <u>system</u> <u>gain</u> must be increased in low-frequency large-amplitude waves to minimize pitch angle variation; but this gain may be decreased in shorter choppy seas. The <u>altitude</u> <u>system</u> <u>gain</u> must also be increased in low-frequency large-amplitude waves because the craft must follow the water to some extent to prevent the foils from broaching. This high altitude gain has two results: (1) it provides a larger signal for the servo to guide the craft up and down with the waves and, (2) it reduces the phase lag between the control signal and the craft response. In high-frequency small-amplitude waves, the craft should approach straight and level flight and a low altitude gain is necessary. This low altitude gain (1) reduces the signal to the servo because it is not necessary or desirable to guide the craft up and down with the waves, and (2) it permits a greater phase lag which is unimportant because of the lower amplitudes of both craft and water surface motion.

An important conclusion of this study is that a definite distinction must be made between guidance and control. In the proposed system the sensing strut is called upon to provide both guidance and control. It is called upon to use the water surface as a guidance reference when the water surface is itself a disturbing input. It now seems that for improved performance the strut should be considered as really suitable only for the guidance function; it should be used only to provide a relatively slow or average measure of water surface position. Relatively fast control against disturbing inputs may have to be provided by an accelerometer which will measure craft accelerations from an inertial space altitude reference.

4.2 Summary of Conclusions

The authors' conclusions can be summarized as follows:

1. Test results indicate better performance than has been previously attained with the Gibbs and Cox craft.

2. By varying gains of the pitch control system and the altitude control system as a function of wavelength, the foils can be kept underneath the water for every sea condition studied.

3. The craft need not follow small-amplitude high-frequency waves, but must begin to follow the water surface as wave amplitude increases and frequency of encounter decreases. Operator control over gain seems necessary.

4. Distinction between guidance and control functions must be emphasized. Results of this thesis indicate that the particular craft studied requires an inertial space reference for altitude. A different configuration or different craft may not need this type of reference.

5. The water vane as simulated did not improve craft performance. The reasons are not clearly understood, but some possible explanations will be discussed in Chapter 5.

6. The authors believe that the craft configuration studied has inherently poor stability characteristics largely because the foil separation is short. The proposed guidance and control system may be quite satisfactory when used on a more stable craft or on a more stable configuration of the present craft.

7. Much fundamental knowledge of hydrofoil behavior remains to be acquired. Continuing basic studies are recommended.

CHAPTER 5

SUGGESTIONS

The authors regret that time limitations have prevented their going further with this study. Many possibilities have suggested themselves; some of the more important ones are listed below in the hope that they may interest or assist future investigators.

1.   In Chapter 4 it was concluded that the control system proposed in this thesis either works or nearly works under most sea conditions tested. It is now suggested that the proposed system might prove considerably more satisfactory if the craft trim altitude were lowered. It is not easy to see the compounded results of running the foil at greater depth. However it is certainly clear that if the foil trims deeper, it can rise further before it broaches.

2.   It is also suggested that performance would probably be improved by increasing the foil separation. It is believed that increased separation will minimize the effect at one foil of a disturbance at the other. This belief is supported by preliminary results of studies now being made by Barnes and Connors of the Flight Control Laboratory.

3.   In the guidance and control system proposed and simulated in this thesis, pitch control was attempted by sending the gyro signal only to the front foil. This in effect meant that the craft rotated about a line through the rear foil. All such rotation involved a translation of the center of gravity. The authors had hoped, but did not have time to try sending gyro signals to both front and rear foils to effect craft rotation about the center of gravity. The signals to the two foils would of course be opposite in sign; and they would have a magnitude ratio determined jointly by the lift characteristics of the two foils and by the distances of the foils from the center of gravity.

The signal from the sensing strut could also be sent to both foils to control altitude. Then if this system was still unsatisfactory, an attempt could be made at achieving a tight loop on altitude by adding an accelerometer at the center of gravity. The accelerometer would provide tight loop control by reference to inertial space, and the strut would provide the slower guidance by reference to an average of the water surface. This would relieve the strut of the difficult task of simultaneously providing slow guidance and fast control.

4. With any control system similar to the one proposed in this thesis, and using a water sensing strut, it will almost certainly be necessary to leave the altitude loop gain under the control of the craft operator. This will permit the operator to adjust the gain to suit the sea conditions – straight and level through small waves, up and over the larger waves.

Also, integral control in the altitude loop might prove advantageous. Investigation is recommended.

5. The authors, again because of time limitations, were unable to investigate their proposal for pitch guidance for following larger waves. It is hoped that others will be able to study it in the future.

6. A great deal remains to be learned about the fundamentals of hydrofoil craft dynamics. Before a good control system can be designed, the craft itself should have as much stability as possible built into it. Work should be continued on such studies as are now in progress at the Flight Control Laboratory. The craft designer should be able to optimize such craft parameters as length of foil separation, radius of gyration, location of center of gravity, trim altitude, etc. The craft designer should have good criteria for the selection of the best hydrofoil section. Also, more should be learned about the seemingly important ratio of foil separation to craft trim velocity.

7. In any frequency analysis of hydrofoil craft, consideration must be given to the difference between a head and following sea. That is, frequency of wave encounter is not the only important quantity. The difference in the phase relationships among water and orbital motions in head and following seas completely changes the situation. However, in random seas, frequency and power spectral density will become the determining factors.

8.   The proposed water vane failed in that it either caused instability or increased the amplitudes of craft responses. Time did not permit investigation of the reasons for failure but the following suggestions are made.

The function desired of the water vane is to measure and give a signal to the servo to correct for change of water velocity direction which is due to orbital motion and to downwash. Reference to Fig. 2-2 shows that the vane actually measures and attempts to wash out these quantities; however it also measures $[\Theta - (\hat{h}/V) + (\dot{\Theta} l_t/V)]$. When the bow of the craft pitches up, the foil angle of attack increases with Θ; this increases the lift at the tail and generates a restoring moment to pitch the craft down again; but the water vane attempts to cancel this effect and therefore cancel the restoring moment. The same kind of effect occurs with the $\dot{h}$ and $\ddot{\Theta}$ terms. The reason for the water vane failure seems to be that the disturbing effects of orbital motion are less important than the stabilizing effects of Θ, $\dot{h}$, and $\ddot{\Theta}$.

It is suggested that the water vane be given further study with particular attention to the effects mentioned above. With an integrating gyro in the system, signals for both Θ and $\dot{\Theta}$ are available. If an accelerometer and integrator were added to the system a signal for $\dot{h}$ would also be available.

It might be useful to add some or all of these signals to the water vane signal — or it might be useful to forget about the water vane. Investigation is recommended.

9.   In some of the sea conditions tested in this study, the foils stayed below the water surface but rotated through large angles with respect to the craft. It is possible that these angles caused the foil to reach the stall angle of attack. Although the question is outside of the scope of this study, it is suggested that a solution might be found by increasing the area of the foil. Investigation is recommended.

APPENDIX A

CHARACTERISTICS OF DEEP WATER WAVES AND
ELECTRONIC SIMULATION

A.1. General Discussion of Water Waves

Undisturbed waves in water take the approximate shape of a trochoid.[12] This is the locus of an inner point of a circle when the circle rolls along a straight line. Its shape is sketched roughly below:
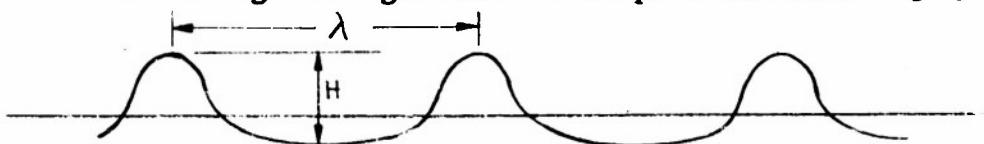
Deep water is defined as the condition where the wave length of the surface wave is less than the depth of the water. When the wave length is less than about one centimeter the wave is described as a ripple. Ocean waves may be as long as one thousand feet and as high as one hundred feet. The horizontal motion of a wave peak is the wave velocity. When waves are moving in the same direction as a surface craft the condition is described as a following sea. When wave and craft velocities are in opposite directions, the condition is a head sea. [Note that the wave velocity with respect to the earth may be either greater or less than the craft velocity with respect to the earth.] When water motion is disturbed by wind, traffic, headlands, etc. the condition may be described as a random sea.[1]

As a wave propagates, water particles move up and down, and they move backward and forward. The resultant motion of a particle is elliptical, decreases exponentially with depth, and is called orbital motion. As a hydrofoil surface moves horizontally, close to the water surface, there is a horizontal water velocity component with respect to the foil. The orbital velocity of water particles adds vectorially to the horizontal velocity. The result is that the effective water velocity over the foil surface is constantly changing both in

magnitude and direction. The very serious effect of this is that the lift and drag forces generated by the foil are also constantly changing. This effect is at its worst in the case of a following sea, because the craft encounters individual waves less frequently and the changes in the forces have a longer time to operate against the inertia of the craft.

A.2. Assumptions Made in this Study

In order to simulate both surface and orbital motion electronically, it is necessary to make certain simplifying assumptions. The assumptions follow.

1. Waves may be represented as sinusoids.

2. Ripples are negligible, and the craft will be operating only in "deep" water.

3. The ratio of wave length to wave height (double-amplitude) lies between 10 and 25.

4. Hydrofoil surface has trim depth of 1.5 chord lengths, or 1.08 feet. Craft is assumed never to approach the surface more closely than 0.9 chordlengths, or 0.648 feet. Any closer approach involves a serious loss of lift and invalidates the mathematical representation. Note however that loss of lift has the desirable effect of causing the craft to settle back into the water.

5. The change due to orbital motion in foil effective angle of attack is sinusoidal and of constant magnitude. The magnitude is calculated as the value for a foil submergence of one foot. This is conservative because of assumption #4 and because this magnitude actually decreases exponentially with submergence.

6. The change due to orbital motion in the magnitude of the water velocity over the foil can be neglected. This is because the effect is much less important than the effect of changing angle of attack, and because the change in magnitude is 90 degrees out of phase with the change in angle. [See Fig. A-1]. The phase relation means that the magnitude effects and the angle effects are never at their worst simultaneously.

7. As angle and magnitude change, there is a lag in buildup of the lift and drag forces. For the craft being studied, this time delay is of the order of 0.002 second.[13] It is therefore neglected.
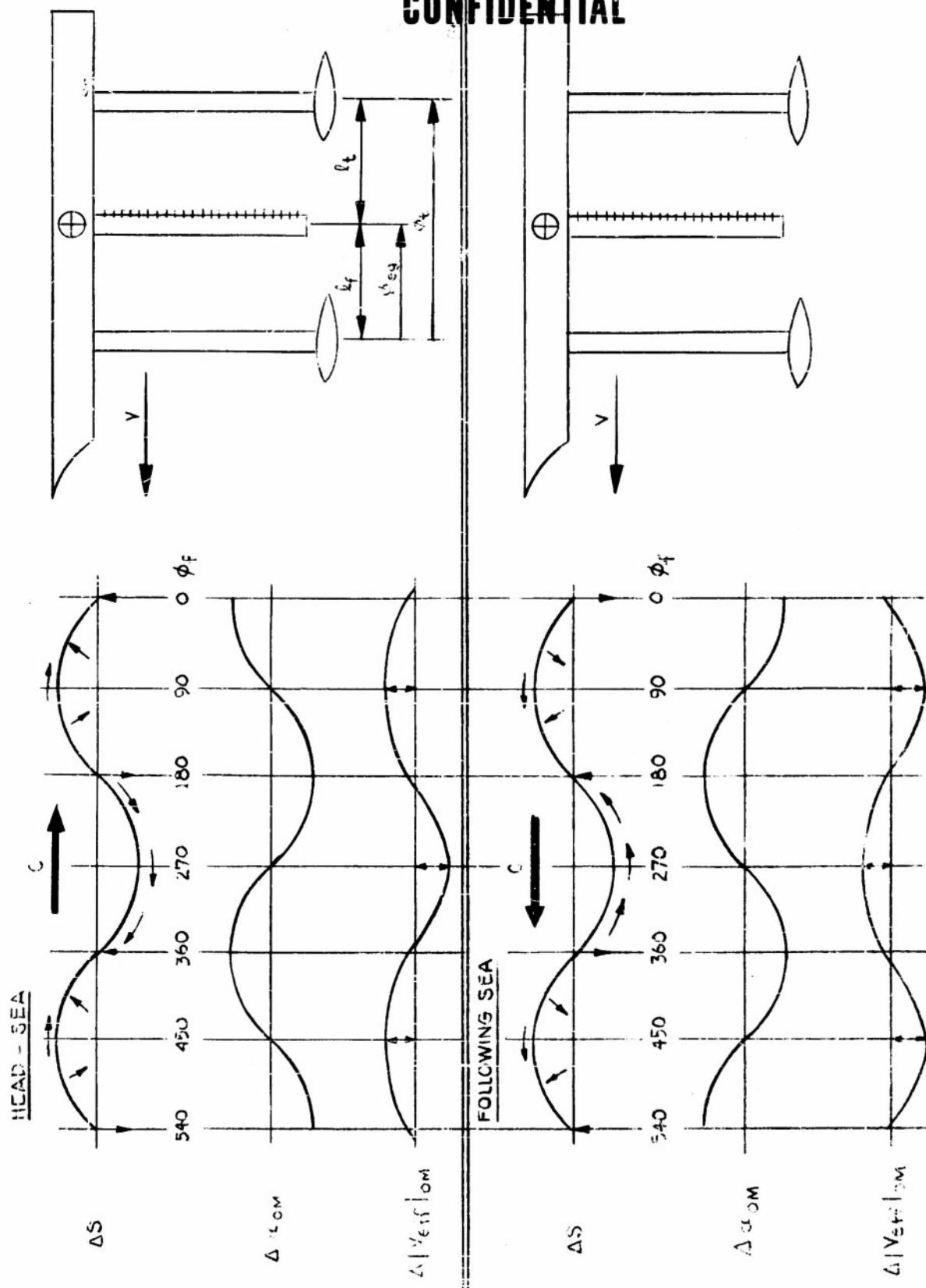
FIG A-1 SEA AND ORBITAL MOTION PHASE RELATIONSHIP

8. Orbital motion is circular, not elliptical.

9. Neither magnitude or phase of tail orbital motion is appreciably affected by downwash.

10. Waves are assumed to have reached sinusoidal steady state. No attempt is made to study transient phenomena.

11. The craft being studied in this thesis certainly should not be expected to cope with waves higher than four feet. Probably the maximum wave should be three feet.

A.3. Water and Orbital Motion Phase Relations

It is not difficult in theory to determine the phase relations among water surface, orbital motion, and craft geometry. In practice it has proved to be confusing, and so one approach will be described in some detail below.

The following definitions are basic:

1. $(\Delta S)_{max}$ is one half the wave height H. ΔS is positive when the water surface is higher than mean water level.

2. $\Delta |V_{eff}|_{OM}$ is the change in the magnitude of the effective water velocity over the hydrofoil surface. $\Delta |V_{eff}|_{OM}$ is positive when it increases the water velocity over the hydrofoil.

3. $\Delta \alpha_{OM}$ is the change in hydrofoil effective angle of attack. $\Delta \alpha_{OM}$ is positive when it causes an increase in upward force.
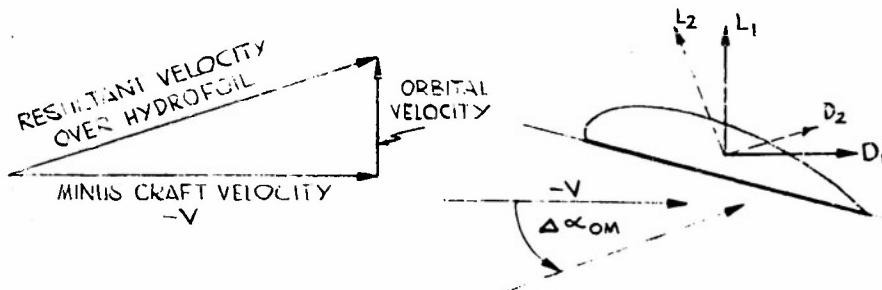
Notice that Lift and Drag vectors rotate with $\Delta \alpha_{OM}$. The change in direction of Lift has a negligible effect on Z forces, and will be neglected. The horizontal component of lift is significant compared with the horizontal component of Drag, and will be accounted for in simulator work.

Figure A-1 shows the various relationships. The small arrows

on the sketch of the water surface show the variation of the orbital motion through the cycle. Note that when orbital motion is directly upward the local angle of attack is such that upward forces are at a maximum; that is, $\Delta\alpha_{OM}$ then has its maximum positive value. Note that $\Delta\alpha_{OM}$ is always 90 degrees in space ahead of ΔS. When observed from the moving craft $\Delta\alpha_{OM}$ can either lag or lead ΔS in time depending on whether there is a following or head sea respectively.

Consider now a head sea and refer to Fig. A-1. The reader is invited to hold the waves still, stand on the front foil, and sail to the left. Define ϕ_f as the number of phase degrees that the boat has sailed toward the left in Fig. A-1. The observer at the front foil will see:

1. A positive peak of $\Delta\alpha_{OM}$ at the front foil when $\phi_f = 0$
2. A positive peak of $\Delta\alpha_{OM}$ reach the rear foil when $\phi_f = \phi_t$
3. A positive peak of ΔS at the front foil when $\phi_f = 90°$
4. A positive peak of ΔS reach the c.g. when $\phi_f = 90° + \phi_{cg}$

That is, in time, $\Delta\alpha_t$ lags $\Delta\alpha_f$ by ϕ_t; and ΔS_{cg} lags $\Delta\alpha_f$ by $(\phi_{cg} + 90°)$. This can be expressed as follows:

$$\Delta\alpha_f = \Delta\alpha_{max} \sin(2\pi ft) \tag{A-1}$$

$$\Delta\alpha_t = \Delta\alpha_{max} \sin(2\pi ft - \phi_t) \tag{A-2}$$

$$\Delta S_{cg} = \Delta S_{cg} \sin(2\pi ft - \phi_{cg} - 90) \tag{A-3}$$

By similar analysis the expressions for a following sea can be found:

$$\Delta\alpha_f = \Delta\alpha_{max} \sin(2\pi ft) \tag{A-4}$$

$$\Delta\alpha_t = \Delta\alpha_{max} \sin(2\pi ft - \phi_t) \tag{A-5}$$

$$\Delta S_{cg} = \Delta S_{max} \sin(2\pi ft - \phi_{cg} + 90) \tag{A-6}$$

A.4. Summary of Relationships

The phase relationships between the water surface and the orbital motion have been described immediately above. Now the following expressions can be verified by reference to the assumptions listed earlier and to Reference 6, Eqs. 1, 2, 3, 4, 12.

$$c = \sqrt{\frac{g\lambda}{2\pi}} = 2.26\sqrt{\lambda} \qquad \text{fps} \tag{A-7}$$

The term $\dot{x}$ is closely related to $\Delta|V_{eff}|_{OM}$, and is small compared with V. Therefore

$$\Delta\alpha_{max} = \frac{\dot{Z}}{-V + \dot{x}} \cong \frac{\dot{Z}}{V} = \frac{V_o}{V} = \frac{H\pi C}{V\lambda} e^{-\frac{2\pi d}{\lambda}} \qquad (A-8)$$

The limited time available for this study has made it necessary to consider only one craft velocity of thirty feet per second. Computer limitations prevent calculating the exponential in (A-8), so a convenient and nearly average depth, d, has been chosen as one foot. The above then becomes:

$$\Delta\alpha_{max} = \frac{0.237\ H}{\sqrt{\lambda}} e^{-\frac{2\pi}{\lambda}} \qquad (A-9)$$

Now consider the frequencies with which the craft will encounter waves

$$f = \frac{V + C}{\lambda} \text{ cps for head sea} \qquad (A-10)$$

$$= \frac{V - C}{\lambda} \text{ cps for following sea} \qquad (A-11)$$

Craft geometry gives:

$$\phi_{cg} = \frac{l_f(2\pi)}{\lambda} = \frac{2018}{\lambda} \text{ degrees} \qquad (A-12)$$

$$\phi_t = \frac{(l_f + l_t)(2\pi)}{\lambda} = \frac{2880}{\lambda} \text{ degrees}$$

Define, for later convenience

$$\sigma = \frac{\Delta\alpha_{max}}{\Delta S_{max}} \qquad (A-13)$$

Recall, for later convenience, the relationship

$$\sin(X + \phi) = \sin X \cos\phi + \cos X \sin\phi \qquad (A-14)$$

When X is a function of time and is a constant, the above becomes

$$\sin(X + \phi) = A \sin X + B \cos X \qquad (A-15)$$

where

$$A = \cos \phi \qquad \text{(A-16)}$$
$$B = \sin \phi \qquad \text{(A-17)}$$

A.5. Simulation of Water and Orbital Motion

In this study, the inputs to the simulator were orbital motion at front and tail foils, and water surface at the sensing strut at the c.g. A sinusoidal output, considered as a cosine wave, was obtained from an ultra-low-frequency oscillator. This wave was put through a phase-shifting device consisting of capacitors and variable resistors. The output of the phase shifter was adjusted until a 90 degree lag was verified by Lissajous figures on a cathode ray oscilloscope. The oscillator output (cosine) and the phase shifter output (sine) were then taken through variable potentiometers to a Sanborn recorder. The sine wave was attentuated by the phase shifter, but the potentiometers made it possible to equalize amplitudes of the two waves. With both a sine and cosine wave available it was possible by using formula (A-15) to obtain a number of sine waves displaced by various phase angles. With these waves considered to have a voltage amplitude analogous to water wave amplitude, ΔS, it was then only necessary to attenuate the amplitude by the factor σ(A-13) to simulate the orbital motion. The procedure is shown schematically in Fig. A-2. The numerical values used are shown in Fig. A-3.
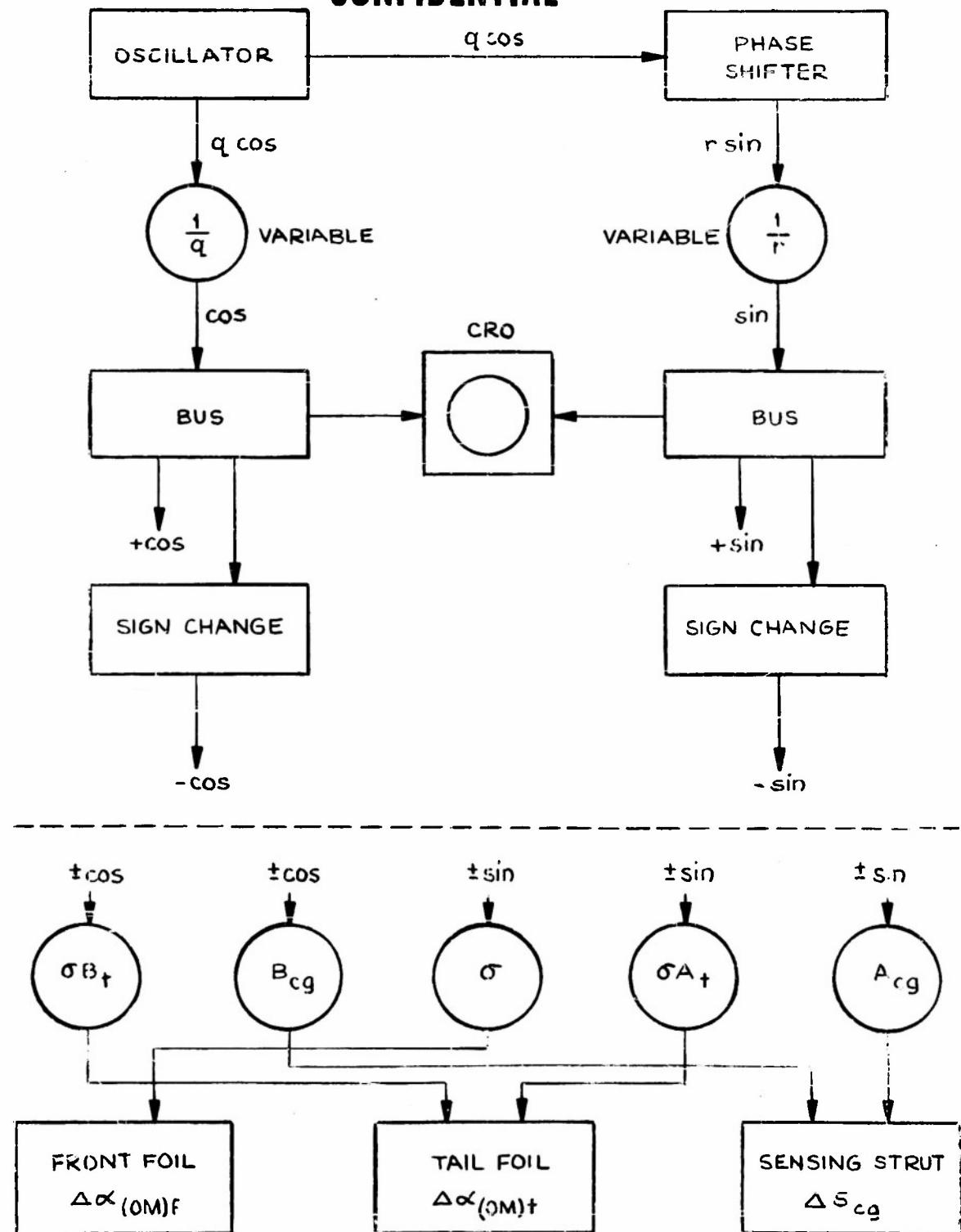
FIG. A-2 SCHEMATIC DIAGRAM OF WATER SIMULATION.

λ ft	C ft/sec	f_{HS} cps	f_{FS} cps	ϕ_{cg} deg	ϕ_t deg	$A_{cg}*$	$B_{cg}*$	σ rad/ft	σ_{A_t} rad/ft	σ_{B_t} rad/ft
5	5.05	7.00	5.0	403	576	-.682	-.731	.0605	-.049	+.0356
10	7.15	3.72	2.29	202	288	+.375	+.927	.08	+.0247	+.0761
15	8.78	2.59	1.42	134	192	-.719	+.695	.0803	-.0785	+.0167
20	10.1	2.05	1.0	101	144	-.982	+.191	.0775	-.0627	-.0455
30	12.4	1.41	0.59	87.2	96	-.920	-.387	.0703	-.0074	-.0698
40	14.3	1.11	0.392	50.5	72	-.772	-.636	.064	+.0198	-.0609
60	17.5	0.792	0.208	33.6	48	-.553	-.833	.0551	+.0368	-.0410
80	20.2	0.628	0.122	25.2	36	-.426	-.905	.0488	+.0396	-.0287

* Note: Signs given with A_{cg} and B_{cg} are for HEAD SEA only.
Change signs of both A_{cg} and B_{cg} for FOLLOWING SEA.

FIG. A-3 TABULATION OF SEA CONDITIONS

APPENDIX B

THE LONGITUDINAL EQUATIONS OF MOTION

The equations of motion are derived by applying Newton's laws of motion for linear and angular acceleration to the hydrofoil craft. The axis system used is a trim axis system, similar to the National Advisory Committee for Aeronautics stability axis system for an aircraft. The system is fixed to the craft and moves with the craft. The X axis lies along the trim velocity vector and is positive in the direction of the velocity vector. The Z axis is positive downward at a right angle to the X axis. The Y axis is at right angles to both the X axis and the Z axis and is positive outward from the starboard side of the craft (see Fig. 2-1).

Restriction of the hydrofoil craft to motions in the plane of symmetry reduces the craft to a three degree of freedom system with three equations of motion. These equations of motion have been developed by Connors[5] for any craft configuration supported by two submerged hydrofoils, one ahead and one behind the center of gravity. Removal of the degree of freedom along the X axis eliminates one of the equations of motion and all terms involving the deviation of the X component of craft velocity from the other two equations. This amounts to the removal of the phygoid (long period) mode. Amster[3] has shown this removal has negligible effects on the short period and on the characteristics of the complete system within the frequency range of interest. Also, Amster has shown that the height derivatives are negligibly small when the submerged foils are operating at least one chord length below the water surface. With these simplifications and with the omission of the strut drag terms and the change in thrust terms, the equations of motion reduce to:[7]

$$Z_{\ddot{\theta}}\,\ddot{\theta} + Z_{\dot{\theta}}\,\dot{\theta} + Z_{\theta}\,\theta + (Z_{\ddot{h}} + m)\,\ddot{h} + Z_{\dot{h}}\,\dot{h} =$$

$$-Z_{\dot{\delta}_f}\,\dot{\delta}_f - Z_{\delta_f}\,\delta_f \qquad\qquad\qquad (B\text{-}1)$$

$$(M_{\ddot{\theta}} - I_y)\,\ddot{\theta} + M_{\dot{\theta}}\,\dot{\theta} + M_{\theta}\,\theta + M_{\ddot{h}}\,\ddot{h} + M_{\dot{h}}\,\dot{h} =$$

$$-M_{\dot{\delta}_f}\,\dot{\delta}_f - M_{\delta_f}\,\delta_f \qquad\qquad\qquad (B\text{-}2)$$

where $(\dot{\ })$ is $d(\ )/dt$, time rate of change of variable.

θ is the change in pitch angle, measured from the horizontal to the X axis and is positive when the craft is tilted bow up and stern down.

h is the change in the height of the center of gravity of the craft from a reference height and is positive when the center of gravity is higher than its reference value.

δ_f is the front foil deflection, and a positive value increases the angle of attack.

I_y is the moment of inertia of the hydrofoil craft about the Y axis.

m is the mass of the craft.

Z_{θ} refers to the force coefficient in the Z direction caused by a change in the pitch angle. Other coefficients are defined in a like manner.

$Z_{\theta}\,\theta$ is the force in pounds in the Z direction caused by a change in the pitch angle. That is, the coefficient multiplied by the quantity in subscript will give the force in pounds.

M_{θ} refers to the moment coefficient about the Y axis caused by a change in the pitch angle.

$M_{\theta}\,\theta$ is the moment in pound-feet about the Y axis caused by a change in the pitch angle.

However, the above equations were developed for a stationary rear foil. The addition of a servo-controlled movable rear foil adds another term to each equation of motion. These terms are $Z_{\delta_t}\delta_t$ and $M_{\delta_t}\delta_t$ and defined later in this appendix as Eqs. (B-12) and (B-22). δ_t is the rear foil deflection, and a positive value increases the angle of attack at the rear foil.

Also, the effects of orbital motion were not included in the above equations. Since orbital motion is a disturbance input to the craft, its effects must be included in the equation of motion. The effect of orbital motion is to introduce an apparent change in the angle of attack at both the front and rear foils. (Refer to Appendix A.) Thus two additional terms, one for orbital motion at the front foil ($\Delta\alpha_{om_f}$) and one for orbital motion at the rear foil ($\Delta\alpha_{om_t}$), must be added to each equation of motion. These terms

$$Z_{\Delta\alpha_{om_f}}\Delta\alpha_{om_f} ,\ Z_{\Delta\alpha_{om_t}}\Delta\alpha_{om_t} ,\ M_{\Delta\alpha_{om_f}}\Delta\alpha_{om_f} ,\ \text{and}\ M_{\Delta\alpha_{om_t}}\Delta\alpha_{om_t}$$

are defined in Eqs. (B-13), (B-14), (B-23) and (B-24).

Now, the resultant equations of motion of the hydrofoil craft are:

$$Z_{\ddot\theta}\ddot\theta + Z_{\dot\theta}\dot\theta + Z_\theta\theta + (Z_{\ddot h}+m)\ddot h + Z_{\dot h}\dot h =$$

$$-Z_{\dot\delta_f}\dot\delta_f - Z_{\delta_f}\delta_f - Z_{\delta_t}\delta_t - Z_{\Delta\alpha_{om_f}}\Delta\alpha_{om_f} - Z_{\Delta\alpha_{om_t}}\Delta\alpha_{om_t} \qquad (B-3)$$

$$(M_{\ddot\theta}-I_y)\ddot\theta + M_{\dot\theta}\dot\theta + M_\theta\theta + M_{\ddot h}\ddot h + M_{\dot h}\dot h =$$

$$-M_{\dot\delta_f}\dot\delta_f - M_{\delta_f}\delta_f - M_{\delta_t}\delta_t - M_{\Delta\alpha_{om_f}}\Delta\alpha_{om_f} - M_{\Delta\alpha_{om_t}}\Delta\alpha_{om_t} \qquad (B-4)$$

where:

$$Z_{\ddot\theta} = S_t \ell \ell_f \frac{\partial\epsilon}{\partial\alpha}N + K_f \frac{\pi}{2}c_f S_f \ell_f - K_t \frac{\pi}{2}c_t S_t \ell_t \qquad (B-5)$$

$$Z_{\dot{\theta}} = -S_t V \left[l_t + \frac{\partial \varepsilon}{\partial \alpha} (l + l_s) \right] N + S_s l_s V \left[\frac{\partial C_L}{\partial \alpha} + C_D \right]_s$$

$$- 2 S_s d_s V C_{L_s} - 2 S_t d_t V C_{L_t} \tag{B-6}$$

$$Z_\theta = - \left[\frac{\partial C_L}{\partial \alpha} + C_D \right]_s S_s V^2 + S_t V^2 N \left[\frac{\partial \varepsilon}{\partial \alpha} - 1 \right] \tag{B-7}$$

$$Z_{\ddot{\lambda}} = S_t l N \frac{\partial \varepsilon}{\partial \alpha} + K_s \frac{\pi}{2} c_s S_s + K_t \frac{\pi}{2} c_t S_t \tag{B-8}$$

$$Z_{\dot{\lambda}} = - \frac{1}{V} Z_\theta \tag{B-9}$$

$$Z_{\dot{\delta}_s} = - S_t l V N \frac{\partial \varepsilon}{\partial \alpha} \tag{B-10}$$

$$Z_{\delta_s} = - S_s V^2 \left[\frac{\partial C_L}{\partial \alpha} \right]_s + S_t V^2 N \frac{\partial \varepsilon}{\partial \alpha} \tag{B-11}$$

$$Z_{\delta_t} = - S_t V^2 \left[\frac{\partial C_L}{\partial \alpha} \right]_t \tag{B-12}$$

$$Z_{\Delta \alpha_{ON_s}} = - S_s V^2 \left[\frac{\partial C_L}{\partial \alpha} + C_D \right]_s + S_t V^2 N \frac{\partial \varepsilon}{\partial \alpha} \tag{B-13}$$

$$Z_{\Delta \alpha_{ON_t}} = - S_t V^2 N \tag{B-14}$$

$$M_{\ddot{\theta}} = - S_t l l_s \left[d_t R - l_t N \right] \frac{\partial \varepsilon}{\partial \alpha} + K_s \frac{\pi}{2} c_s S_s l_s \left[\frac{c_s}{4} - l_s \right]$$

$$- K_t \frac{\pi}{2} c_t S_t l_t \left[\frac{c_t}{4} + l_t \right] \tag{B-15}$$

$$M_{\dot{\theta}} = - S_s V l_s d_s \left[C_L - \frac{\partial C_D}{\partial \alpha} \right]_s - S_s V l_s^2 \left[\frac{\partial C_L}{\partial \alpha} + C_D \right]$$

$$+ S_t V \left[l_t + \frac{\partial \varepsilon}{\partial \alpha} (l + l_s) \right] \left[d_t R - l_t N \right] + 2 S_s V d_s \left[l_s C_{L_s} - d_s C_{D_s} \right]$$

$$+ 2 S_t V d_t \left[- l_t C_{L_t} - d_t C_{D_t} \right] \tag{B-16}$$

$$M_\theta = S_s V^2 d_s \left[C_L - \frac{\partial C_D}{\partial \alpha} \right]_s + S_s V^2 l_f \left[\frac{\partial C_L}{\partial \alpha} + C_D \right]_f$$
$$+ S_t V^2 \left[1 - \frac{\partial \varepsilon}{\partial \alpha} \right] \left[d_t R - l_t N \right] \tag{B-17}$$

$$M_{\ddot{\lambda}} = -S_t l \left[d_t R - l_t N \right] \frac{\partial \varepsilon}{\partial \alpha} + K_s \frac{\pi}{2} c_s S_s \left[\frac{c_s}{4} - l_s \right]$$
$$+ K_t \frac{\pi}{2} c_t S_t \left[\frac{c_t}{4} + l_t \right] \tag{B-18}$$

$$M_{\dot{\lambda}} = -\frac{1}{V} M_\theta \tag{B-19}$$

$$M_{\dot{\delta}_s} = S_t V l \left[d_t R - l_t N \right] \frac{\partial \varepsilon}{\partial \alpha} \tag{B-20}$$

$$M_{\delta_s} = -S_s V^2 d_s \left[\frac{\partial C_D}{\partial \alpha} \right]_s + S_s V^2 l_s \left[\frac{\partial C_L}{\partial \alpha} \right]_s$$
$$- S_t V^2 \left[d_t R - l_t N \right] \frac{\partial \varepsilon}{\partial \alpha} \tag{B-21}$$

$$M_{\delta_t} = -S_t V^2 l_t \left[\frac{\partial C_L}{\partial \alpha} \right]_t - S_t V^2 d_t \left[\frac{\partial C_D}{\partial \alpha} \right]_t \tag{B-22}$$

$$M_{\Delta \alpha_{oM_f}} = S_s V^2 d_s \left[C_L - \frac{\partial C_D}{\partial \alpha} \right]_s + S_s V^2 l_s \left[\frac{\partial C_L}{\partial \alpha} + C_D \right]_s$$
$$+ S_t V^2 \left[l_t N - d_t R \right] \left[\frac{\partial \varepsilon}{\partial \alpha} \right] \tag{B-23}$$

$$M_{\Delta \alpha_{oM_t}} = S_t V^2 \left[d_t R - l_t N \right] \tag{B-24}$$

$$I_y = m \, r_{gy}^2 \tag{B-25}$$

$$R = \left[\frac{\partial C_L}{\partial \alpha} \right]_t \left[\alpha_t - 2 \varepsilon_{TRIM} \right] - \left[\frac{\partial C_D}{\partial \alpha} \right]_t \tag{B-26}$$

$$N = \left[\frac{\partial C_L}{\partial \alpha}\right]_t + C_{D_t} - \epsilon_{TRIM}\left[\frac{\partial C_D}{\partial \alpha}\right]_t \qquad (B-27)$$

It may be important to note that the effects of time lag in force buildup on the hydrofoils has been neglected. When a foil is suddenly deflected, a finite time interval elapses before the new flow pattern is established. The small amount of experimental work with these delays has indicated that the time lag is negligible. [13]

APPENDIX C

DERIVATION OF THE LONGITUDINAL RELATING FUNCTIONS OF THE HYDROFOIL

C.1 General procedure and assumptions

The relating functions of main interest in this thesis are those of the craft itself because they are a consequence of the basic physical relationships and are necessarily present in the analysis. These functions relate pitch angle and height to elevator and wave motion.

The relating functions are obtained by taking the Laplace Transform of the equations of motion (B-3) and (B-4) with zero initial conditions, and solving the resulting determinant for the desired relating functions, where $[RF]_{(\quad)[q\ in;\ q\ out]}$ is defined as the ratio of two polynomials in the Laplace transform p, with p equal to the complex number $\alpha + jw$. For the steady-state frequency analysis used in this thesis, the real part of p is zero, so that p = jw.

The transformed function usually carries a superscript establishing it as a function of p, but in this thesis the notation is dropped to avoid any confusion with vector notation. It should be assumed, therefore, that variables appearing in equations as Laplace transform p, represent transformed variables.

C.2 Summary of short period mode longitudinal relating functions

The relating functions are:

$$h = [RF]_{(H)[\delta_f;\ h]}\ \delta_f \tag{C-1}$$

$$h = [RF]_{(H)[\delta_t;\ h]}\ \delta_t \tag{C-2}$$

$$\dot{h} = [RF]_{(H)[\Delta\alpha_{OM_f};h]} \, \Delta\alpha_{OM_f} \tag{C-3}$$

$$h = [RF]_{(H)[\Delta\alpha_{OM_t};h]} \, \Delta\alpha_{OM_t} \tag{C-4}$$

$$\theta = [RF]_{(H)[\delta_f;\theta]} \, \delta_f \tag{C-5}$$

$$\theta = [RF]_{(H)[\delta_t;\theta]} \, \delta_t \tag{C-6}$$

$$\theta = [RF]_{(H)[\Delta\alpha_{OM_f};\theta]} \, \Delta\alpha_{OM_f} \tag{C-7}$$

$$\theta = [RF]_{(H)[\Delta\alpha_{OM_t};\theta]} \, \Delta\alpha_{OM_t} \tag{C-8}$$

$$[RF]_{(H)[\delta_f;\theta]} = \frac{S_{\theta_1}\left[\frac{p^2}{\omega_{n\theta_1}^2} + \frac{2\zeta_{n\theta_1}}{\omega_{n\theta_1}}p + 1\right]}{p\left[\frac{p^2}{\omega_{n_H}^2} + \frac{2\zeta_{n_H}}{\omega_{n_H}}p + 1\right]} \tag{C-9}$$

$$[RF]_{(H)[\delta_t;\theta]} = \frac{S_{\theta_2}\left[\tau_{\theta_2}p + 1\right]}{p\left[\frac{p^2}{\omega_{n_H}^2} + \frac{2\zeta_{n_H}}{\omega_{n_H}}p + 1\right]} \tag{C-10}$$

$$[RF]_{(H)[\Delta\alpha_{OM_f};\theta]} = \frac{S_{\theta_3}\left[\tau_{\theta_3}p + 1\right]}{p\left[\frac{p^2}{\omega_{n_H}^2} + \frac{2\zeta_{n_H}}{\omega_{n_H}}p + 1\right]} \tag{C-11}$$

$$[RF]_{(H)[\Delta\alpha_{OM_t};\theta]} = \frac{S_{\theta_4}\left[\tau_{\theta_4}p + 1\right]}{p\left[\frac{p^2}{\omega_{n_H}^2} + \frac{2\zeta_{n_H}}{\omega_{n_H}}p + 1\right]} \tag{C-12}$$

$$[RF]_{(H)[\delta_s;h]} = \frac{S_{h_1}\left[a_0 p^3 + a_1 p^2 + a_2 p + 1\right]}{p^2\left[\frac{p^2}{\omega_{n_H}^2} + \frac{2J_{n_H}}{\omega_{n_H}}p + 1\right]} \tag{C-13}$$

$$[RF]_{(H)[\delta_t;h]} = \frac{S_{h_2}\left[\frac{p^2}{\omega_{n_{h_2}}^2} + \frac{2J_{n_{h_2}}}{\omega_{n_{h_2}}}p + 1\right]}{p^2\left[\frac{p^2}{\omega_{n_H}^2} + \frac{2J_{n_H}}{\omega_{n_H}}p + 1\right]} \tag{C-14}$$

$$[RF]_{(H)[\Delta\alpha_{om_3};h]} = \frac{S_{h_3}\left[\frac{p^2}{\omega_{n_{h_3}}^2} + \frac{2J_{n_{h_3}}}{\omega_{n_{h_3}}}p + 1\right]}{p^2\left[\frac{p^2}{\omega_{n_H}^2} + \frac{2J_{n_H}}{\omega_{n_H}}p + 1\right]} \tag{C-15}$$

$$[RF]_{(H)[\Delta\alpha_{om_4};h]} = \frac{S_{h_4}\left[\frac{p^2}{\omega_{n_{h_4}}^2} + \frac{2J_{n_{h_4}}}{\omega_{n_{h_4}}}p + 1\right]}{p^2\left[\frac{p^2}{\omega_{n_H}^2} + \frac{2J_{n_H}}{\omega_{n_H}}p + 1\right]} \tag{C-16}$$

where:

$$S_{\theta_1} = \frac{M_{\dot{h}} Z_{\delta_s} - M_{\delta_s} Z_{\dot{h}}}{(Z_{\ddot{h}}+m)M_\theta + M_{\dot{\theta}} Z_{\dot{h}} - M_{\ddot{h}} Z_\theta - M_{\dot{h}} Z_{\dot{\theta}}} \tag{C-17}$$

$$S_{\theta_2} = \frac{M_{\dot{h}} L_{\delta_t} - M_{\delta_t} Z_{\dot{h}}}{(Z_{\ddot{h}}+m)M_\theta + M_{\dot{\theta}} Z_{\dot{h}} - M_{\ddot{h}} Z_\theta - M_{\dot{h}} Z_{\dot{\theta}}} \tag{C-18}$$

$$S_{\theta_3} = \frac{M_{\dot{h}} Z_{\Delta\alpha_{om_3}} - M_{\Delta\alpha_{om_3}} Z_{\dot{h}}}{(Z_{\ddot{h}}+m)M_\theta + M_{\dot{\theta}} Z_{\dot{h}} - M_{\ddot{h}} Z_\theta - M_{\dot{h}} Z_{\dot{\theta}}} \tag{C-19}$$

$$S_{\theta_4} = \frac{M_{\dot{h}} Z_{\Delta\alpha_{om_4}} - M_{\Delta\alpha_{om_4}} Z_{\dot{h}}}{(Z_{\ddot{h}}+m)M_\theta + M_{\dot{\theta}} Z_{\dot{h}} - M_{\ddot{h}} Z_\theta - M_{\dot{h}} Z_{\dot{\theta}}} \tag{C-20}$$

$$\zeta_{n_{\theta_1}} = \frac{\omega_{n_{\theta_1}}}{2}\left[\frac{M_{\ddot{\imath}}Z_{\dot{\delta}_5}+M_{\ddot{\imath}}Z_{\delta_5}-M_{\dot{\delta}_5}Z_{\ddot{\imath}}-(Z_{\ddot{\imath}}+m)M_{\delta_5}}{M_{\ddot{\imath}}Z_{\delta_5}-M_{\delta_5}Z_{\ddot{\imath}}}\right] \tag{C-21}$$

$$\omega_{n_{\theta_1}} = \sqrt{\frac{M_{\ddot{\imath}}Z_{\delta_5}-M_{\delta_5}Z_{\ddot{\imath}}}{M_{\ddot{\imath}}Z_{\dot{\delta}_5}-(Z_{\ddot{\imath}}+m)M_{\dot{\delta}_5}}} \tag{C-22}$$

$$\tau_{\theta_2} = \frac{M_{\ddot{\imath}}Z_{\delta_e}-(Z_{\ddot{\imath}}+m)M_{\delta_e}}{M_{\ddot{\imath}}Z_{\delta_e}-M_{\delta_e}Z_{\ddot{\imath}}} \tag{C-23}$$

$$\tau_{\theta_3} = \frac{M_{\ddot{\imath}}Z_{\Delta\alpha_{OMS}}-(Z_{\ddot{\imath}}+m)M_{\Delta\alpha_{OMS}}}{M_{\ddot{\imath}}Z_{\Delta\alpha_{OMS}}-Z_{\ddot{\imath}}M_{\Delta\alpha_{OMS}}} \tag{C-24}$$

$$\tau_{\theta_4} = \frac{M_{\ddot{\imath}}Z_{\Delta\alpha_{OMe}}-(Z_{\ddot{\imath}}+m)M_{\Delta\alpha_{OMe}}}{M_{\ddot{\imath}}Z_{\Delta\alpha_{OMe}}-Z_{\ddot{\imath}}M_{\Delta\alpha_{OMe}}} \tag{C-25}$$

$$S_{\kappa_1} = \frac{M_{\delta_5}Z_{\theta}-M_{\theta}Z_{\delta_5}}{(Z_{\ddot{\imath}}+m)M_{\theta}+M_{\theta}Z_{\ddot{\imath}}-M_{\ddot{\imath}}Z_{\theta}-M_{\ddot{\imath}}Z_{\dot{\theta}}} \tag{C-26}$$

$$S_{\kappa_2} = \frac{M_{\delta_e}Z_{\theta}-M_{\theta}Z_{\delta_e}}{(Z_{\ddot{\imath}}+m)M_{\theta}+M_{\dot{\theta}}Z_{\ddot{\imath}}-M_{\ddot{\imath}}Z_{\theta}-M_{\ddot{\imath}}Z_{\dot{\theta}}} \tag{C-27}$$

$$S_{\kappa_3} = \frac{M_{\Delta\alpha_{OMS}}Z_{\theta}-M_{\theta}Z_{\Delta\alpha_{OMS}}}{(Z_{\ddot{\imath}}+m)M_{\theta}+M_{\theta}Z_{\ddot{\imath}}-M_{\ddot{\imath}}Z_{\theta}-M_{\ddot{\imath}}Z_{\dot{\theta}}} \tag{C-28}$$

$$S_{\kappa_4} = \frac{M_{\Delta\alpha_{OMe}}Z_{\theta}-M_{\theta}Z_{\Delta\alpha_{OMe}}}{(Z_{\ddot{\imath}}+m)M_{\theta}+M_{\dot{\theta}}Z_{\ddot{\imath}}-M_{\ddot{\imath}}Z_{\theta}-M_{\ddot{\imath}}Z_{\dot{\theta}}} \tag{C-29}$$

$$a_o = \frac{M_{\dot{\delta}_f} Z_{\ddot{\theta}} - (M_{\ddot{\theta}} - I_y) Z_{\dot{\delta}_f}}{M_{\delta_f} Z_{\theta} - M_{\theta} Z_{\delta_f}}$$

(C-30)

$$a_1 = \frac{M_{\delta_f} Z_{\ddot{\theta}} - (M_{\ddot{\theta}} - I_y) Z_{\delta_f} + M_{\dot{\delta}_f} Z_{\dot{\theta}} - M_{\dot{\theta}} Z_{\dot{\delta}_f}}{M_{\delta_f} Z_{\theta} - M_{\theta} Z_{\delta_f}}$$

(C-31)

$$a_2 = \frac{M_{\delta_f} Z_{\dot{\theta}} + M_{\dot{\delta}_f} Z_{\theta} - M_{\dot{\theta}} Z_{\delta_f} - M_{\theta} Z_{\dot{\delta}_f}}{M_{\delta_f} Z_{\theta} - M_{\theta} Z_{\delta_f}}$$

(C-32)

$$\omega_{n_{\lambda_2}} = \sqrt{\frac{Z_{\theta} M_{\delta_t} - M_{\theta} Z_{\delta_t}}{M_{\delta_t} Z_{\ddot{\theta}} - (M_{\ddot{\theta}} - I_y) Z_{\dot{\delta}_t}}}$$

(C-33)

$$\mathcal{J}_{n_{\lambda_2}} = \frac{\omega_{n_{\lambda_2}}}{2} \left[\frac{M_{\delta_t} Z_{\dot{\theta}} - M_{\dot{\theta}} Z_{\delta_t}}{M_{\delta_t} Z_{\theta} - M_{\theta} Z_{\delta_t}} \right]$$

(C-34)

$$\omega_{n_{\lambda_3}} = \sqrt{\frac{Z_{\theta} M_{\Delta\alpha_{oM_f}} - M_{\theta} Z_{\Delta\alpha_{oM_f}}}{Z_{\ddot{\theta}} \dot{M}_{\Delta\alpha_{oM_f}} - (M_{\ddot{\theta}} - I_y) Z_{\Delta\alpha_{oM_f}}}}$$

(C-35)

$$\mathcal{J}_{n_{\lambda_3}} = \frac{\omega_{n_{\lambda_3}}}{2} \left[\frac{M_{\Delta\alpha_{oM_f}} Z_{\dot{\theta}} - M_{\dot{\theta}} Z_{\Delta\alpha_{oM_f}}}{M_{\Delta\alpha_{oM_f}} Z_{\theta} - M_{\theta} Z_{\Delta\alpha_{oM_f}}} \right]$$

(C-36)

$$\omega_{n_{\lambda_4}} = \sqrt{\frac{Z_{\theta} M_{\Delta\alpha_{oM_t}} - M_{\theta} Z_{\Delta\alpha_{oM_t}}}{Z_{\ddot{\theta}} M_{\Delta\alpha_{oM_t}} - (M_{\ddot{\theta}} - I_y) Z_{\Delta\alpha_{oM_t}}}}$$

(C-37)

$$\mathcal{J}_{n_{\lambda_4}} = \frac{\omega_{n_{\lambda_4}}}{2} \left[\frac{M_{\Delta\alpha_{oM_t}} Z_{\dot{\theta}} - M_{\dot{\theta}} Z_{\Delta\alpha_{oM_t}}}{M_{\Delta\alpha_{oM_t}} Z_{\theta} - M_{\theta} Z_{\Delta\alpha_{oM_t}}} \right]$$

(C-38)

$$\omega_{n_H} = \sqrt{\frac{(Z_{\dot{x}} + m)M_\theta + Z_{\dot{x}}M_{\dot{\theta}} - M_{\dot{x}}\overline{Z_{\dot{\theta}}} - M_{\dot{x}}Z_\theta}{(Z_{\dot{x}} + m)(M_{\ddot{\theta}} - I_y) - M_{\dot{x}}Z_{\ddot{\theta}}}} \qquad \text{(C-39)}$$

$$\mathcal{J}_{n_H} = \frac{\omega_{n_H}}{2}\left[\frac{(Z_{\dot{x}} + m)M_{\dot{\theta}} + (M_{\ddot{\theta}} - I_y)Z_{\dot{x}} - Z_{\ddot{\theta}}M_{\dot{x}} - Z_{\dot{\theta}}M_{\ddot{x}}}{(Z_{\dot{x}} + m)M_\theta + M_{\dot{\theta}}Z_{\dot{x}} - M_{\dot{x}}Z_{\dot{\theta}} - M_{\dot{x}}Z_\theta}\right] \qquad \text{(C-40)}$$

In calculating the hydrofoil characteristic equation parameters (C-39) and (C-40), use is made of the relation $M_\theta Z_{\dot{h}} - M_{\dot{h}}Z_\theta \equiv 0$ which is seen to hold from the definitions of the stability derivatives in Appendix B.

The relating functions as stated above apply to the system as studied on the Flight Control Laboratory Analog Computer. It should be noted, however, that in Eqs. (C-9) and (C-13), the numerator is only one order lower than the denominator. This representation, a slight departure from the entire physical picture, arises because some terms are omitted from the original equations of motion. A change in front foil deflection causes changes in forces at the rear foil. Some terms in the equations describe the magnitude of these force changes; these terms have been retained. Other terms describe the time delay between a front foil deflection and its effect at the rear foil; these terms have been omitted. The result of retaining some terms of the equations of motion while neglecting certain other corresponding terms is that no factor expressing the force change time delay appears in the denominator of the relating function. For a more consistent view, either the front foil deflection rate terms could be removed, or else the force change lag retained. Since in any event the terms added or removed have been found to be small, the effect of any of these changes will be insignificant.

APPENDIX D

CLOSED LOOP CONTROL SYSTEM AND LONGITUDINAL MODE
HYDROFOIL PERFORMANCE

General procedure

The method adopted for analysis of the closed loop control system of the longitudinal mode is to divide the system into loops, analyze each loop separately, then combine the results and apply inputs to get the closed-loop system responses. Since the altitude-control loop is unstable by itself, the tight-loop pitch-control system must be functioning in order to study the height response of the craft on the simulator.

Steady-state sinusoidal frequency techniques are employed in this appendix. This basic procedure is described in any standard text on the subject.[16]

To check the system on the computer, the pitch-control loop point of neutral stability is determined with the altitude – control loop disconnected. Then with a chosen value of gain in the pitch-control loop and both loops connected, the total system is brought to the neutral point. This gives a one-point check on the overall computer wiring connections.

Numerical values of parameters used

The numerical values of the Gibbs and Cox craft are included in Table D-1. These values are used in this thesis.

Some of the relating functions defined in Appendix C show second-order factors. These particular values of parameters in Table D-1 result in $f > 1$ for some of the second-order factors. In these cases, the second-order factors break down into two first-order factors, but the general definitions as second-order factors are still valid.

TABLE D-1

V_{craft}	30 ft/sec	W	3,000 lb
$Z_{\ddot{\theta}}$	143 lb/rad/sec^2	$(I_y - M_{\ddot{\theta}})$	3236 lb ft/rad/sec^2
$Z_{\dot{\theta}}$	−1,920 lb/rad/sec	$M_{\dot{\theta}}$	−24,000 lb ft/rad/sec
Z_{θ}	−42,600 lb/rad	M_{θ}	15,700 lb ft/rad
$(Z_{\ddot{h}} + m)$	131 lb/ft/sec^2	$M_{\ddot{h}}$	56.3 lb ft/ft/sec^2
$Z_{\dot{h}}$	1,421 lb/ft/sec	$M_{\dot{h}}$	−524 lb ft/ft/sec
$Z_{\dot{\delta}_f}$	−751 lb/rad/sec	$M_{\dot{\delta}_f}$	−1,709 lb ft/rad/sec
Z_{δ_f}	−11,300 lb/rad	M_{δ_f}	83,500 lb ft/rad
Z_{δ_t}	−31,700 lb/rad	M_{δ_t}	−79,600 lb ft/rad
$Z_{\Delta\infty OM_f}$	−11,200 lb/rad	$M_{\Delta\infty OM_f}$	87,200 lb ft/rad
$Z_{\Delta\infty OM_t}$	−31,300 lb/rad	$M_{\Delta\infty OM_t}$	−71,200 lb ft/rad
ℓ_f	5.6 ft	$\omega_{n_{fs}}$	30 rad/sec
ℓ_t	2.4 ft	$\omega_{n_{rs}}$	30 rad/sec
ℓ	8.0 ft	$\gamma_{n_{fs}}$	0.7
c	0.721 ft	$\gamma_{n_{rs}}$	0.7
$r_{(gy)}$	6.0 ft	τ_{sm}	0.01 sec
d_f	3.75 ft	$d_{submergence}$	1.5 c
d_t	3.75 ft	A_f	7.5
S_f	3.91 ft^2	A_t	15.0
S_t	7.82 ft^2		

Pitch control system gain-phase diagram

The simplest method of applying ordinary servo techniques of analysis to this system is to separate the loops. The gyro-monitored pitch-control loop is considered first. When analyzing this pitch-control system, the altitude-control loop and its associated components are disconnected from the system.

Figure (D-1) is an open loop amplitude-phase plot with frequency as a parameter. It can be used to check the computer by increasing the loop gain on a potentiometer of the computer until the system becomes neutrally stable. The frequency of oscillation of the system corresponds to the frequency of crossover (where the phase angle equals minus 180 degrees). The value of gain on the potentiometer corresponds to the value of gain necessary to displace the curve of Fig. (D-1) to the right so that the crossover frequency coincides with an amplitude ratio of unity. This is the point of neutral stability, where the open loop relating function equals minus one (the denominator of the closed-loop relating function goes to zero). If the frequencies and the gains from the computer and from the gain-phase diagram are equal, it is an indication that the problem is being simulated correctly at least at the higher frequencies.

Pitch control system

Pitch angle is to be maintained by deflecting the front foil in response to commands from a single-degree-of-freedom integrating gyro. Other components in the loop which are necessary to accomplish this control are a front foil servo and a lead-lag signal modifier network. Performance of these components is best described by specifying their relating functions.

$$\left[RF\right]_{(GU)[\theta;\,e]} = S_{(GU)} \tag{D-1}$$

$$\left[RF\right]_{(SM)[e;\,e]} = S_{(SM)} \left[\frac{\propto \tau_{(SM)}\,p + 1}{\tau_{(SM)}\,p + 1}\right] \tag{D-2}$$
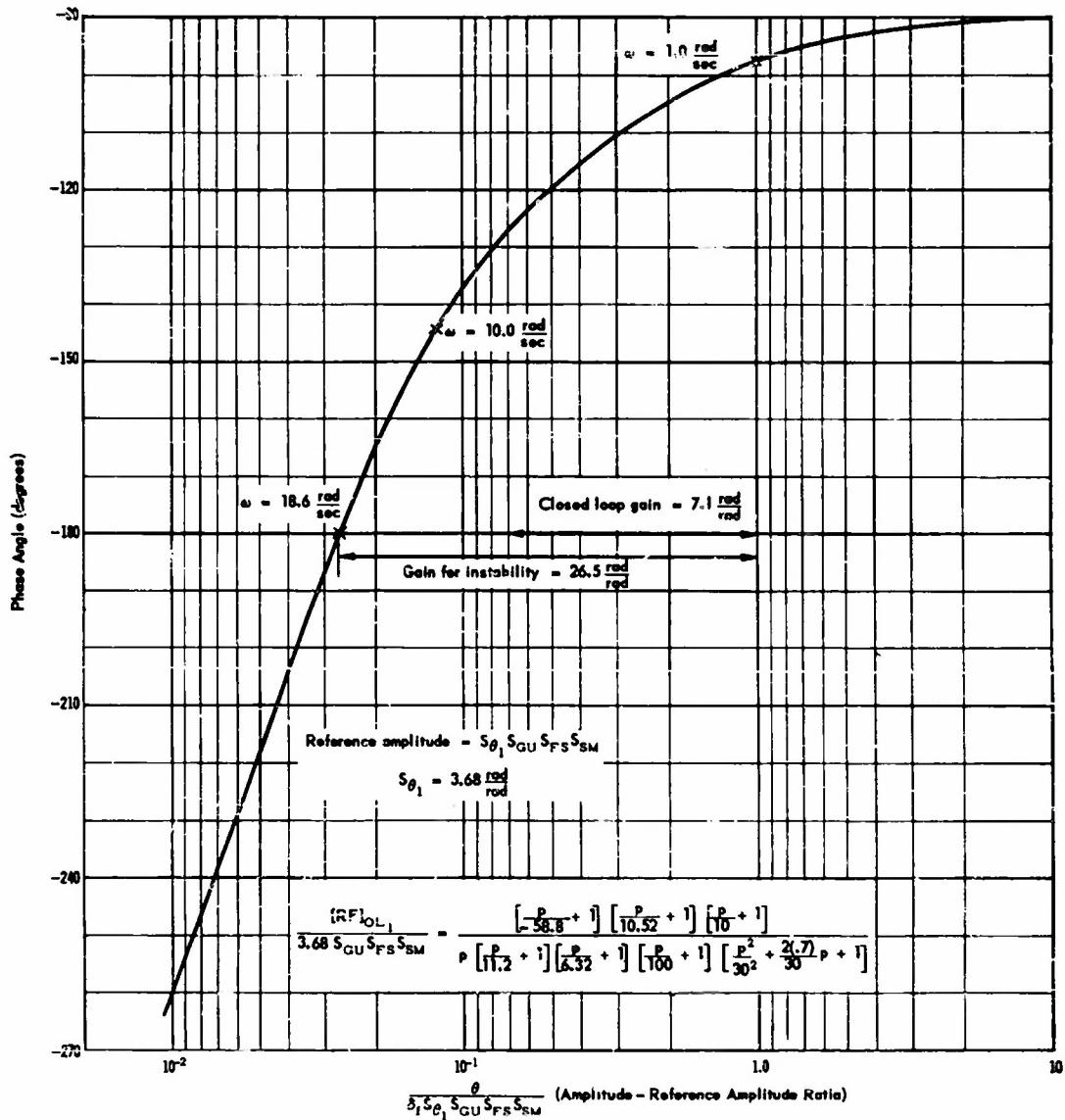
Fig. D-1. Gain-phase diagram for pitch control loop.

$$[RF]_{(FS)[e;\delta_f]} = S_{(FS)} \frac{1}{\left[\frac{P^2}{\omega_{n_{FS}}^2} + \frac{2\mathcal{T}_{nFS}}{\omega_{n_{FS}}}P + 1\right]} \tag{D-3}$$

From Eqs. (C-9) and (C-11):

$$[RF]_{(H)[\delta_f;\theta]} = \frac{S_{\theta_1}\left[\left(\frac{P}{\omega_{n_{\theta_1}}}\right)^2 + \frac{2\mathcal{T}_{n\theta_1}}{\omega_{n_{\theta_1}}}P + 1\right]}{P\left[\left(\frac{P}{\omega_{n_H}}\right)^2 + \frac{2\mathcal{T}_{nH}}{\omega_{n_H}}P + 1\right]} \tag{C-9}$$

$$[RF]_{(H)[\Delta\alpha_{on};\theta]} = \frac{S_{\theta_S}\left[\tau_{\theta_S}P + 1\right]}{P\left[\left(\frac{P}{\omega_{n_H}}\right)^2 + \frac{2\mathcal{T}_{nH}}{\omega_{n_H}}P + 1\right]} \tag{C-11}$$

The open loop relating function is:

$$[RF]_{(OL)_1} = [RF]_{(H)[\delta_f;\theta]}[RF]_{(\delta\sigma)[\theta;e]}[RF]_{(\delta S)[e;c]}[RF]_{(FS)[e;\delta]} \tag{D-4}$$

By looking at the functional diagram, Fig. (2-2), it is seen that the closed loop relating function for an orbital motion input on the front foil and pitch angle output is:

$$[RF]_{(FCS)[\Delta\alpha_{on};\theta]} = \frac{[RF]_{(H)[\Delta\alpha_{on};\theta]}}{1 + [RF]_{(OL)_1}} \tag{D-5}$$

Response of the pitch control system to steady-state sinusoidal orbital motion inputs is shown in Figs. (D-2) and (D-3) where the response is plotted as a function of frequency.

A frequently used criterion for good system performance is that the peak amplitude shall not be greater than 1.3 times the amplitude at very low frequencies. The best value of open loop gain found experimentally corresponds very closely to the gain determined analytically as necessary to meet this 1.3 criterion. This experimental value of gain $(S_{(OL)_1} = 7.1)$ was used in the closing of the pitch control loop.

A further use of the closed loop response in Figs. (D-2) and (D-3) is to completely check the computer response of the pitch control system. This is accomplished by putting sinusoidal disturbing inputs on the front foil and comparing the computer oscillograph record of pitch angle and input orbital motion amplitude (for a particular frequency) with the corresponding point on the analytical solution of Figs. (D-2) and (D-3). The advantage of this check is that it can be used over the entire frequency range.

Altitude control system

Altitude is to be maintained by a deflection of the rear foil in response to commands received from a strut located at the center of gravity of the craft. The other component in the altitude control loop necessary to accomplish this control is a rear foil servo. These components can be described by the following relating functions:

$$\left[KF \right]_{[strut]} = S_{(SE)} \tag{D-6}$$

$$\left[KF \right]_{[foil servo]} = \frac{S_{(RS)} \left[\dfrac{1}{\left[\left(\dfrac{P}{\omega_{h_{RS}}} \right)^2 + \dfrac{2 J_{h_{RS}}}{\omega_{r_{RS}}} P + 1 \right]} \right]} \tag{D-7}$$

The relating function (C-14) of the hydrofoil craft for a rear foil deflection input and a deviation in height output is unstable. However, by closing the pitch control loop and considering the pitch control system as a
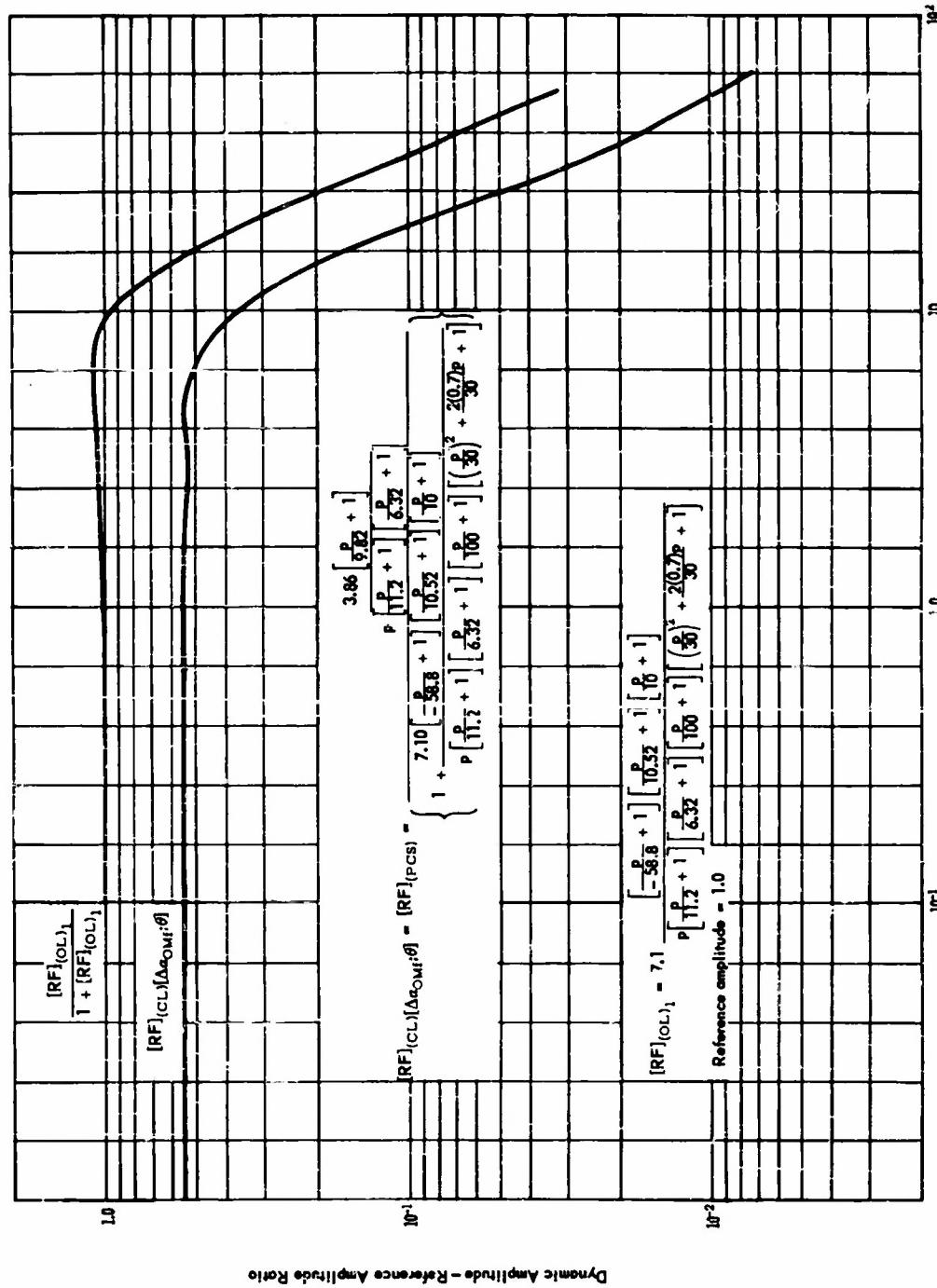
Fig. D-2. Steady state frequency response of the pitch control loop.

$$\frac{[RF]_{(OL)_1}}{1 + [RF]_{(OL)_1}}$$

$$[RF]_{(CL)}[\Delta\alpha_{OM};\theta]$$

$$[RF]_{(CL)}[\Delta\alpha_{OM};\theta] = [RF]_{(PCS)} = \frac{3.86\left[\frac{P}{9.62}+1\right]}{P\left[\frac{P}{11.2}+1\right]\left[\frac{P}{10.52}+1\right]\left[\frac{P}{6.32}+1\right]\left[\frac{P}{100}+1\right]\left[\frac{P}{70}+1\right]}$$

$$1 + \frac{7.10\left[\frac{-P}{58.8}+1\right]}{P\left[\frac{P}{11.2}+1\right]\left[\frac{P}{6.32}+1\right]\left[\frac{P}{100}+1\right]\left[\left(\frac{P}{30}\right)^2+\frac{2(0.7)P}{30}+1\right]}$$

$$[RF]_{(OL)_1} = 7.1 \frac{\left[\frac{-P}{58.8}+1\right]\left[\frac{P}{10.52}+1\right]\left[\frac{P}{70}+1\right]}{P\left[\frac{P}{11.2}+1\right]\left[\frac{P}{6.32}+1\right]\left[\frac{P}{100}+1\right]\left[\left(\frac{P}{30}\right)^2+\frac{2(0.7)P}{30}+1\right]}$$

Reference amplitude = 1.0

Frequency (radians/second)

Dynamic Amplitude – Reference Amplitude Ratio
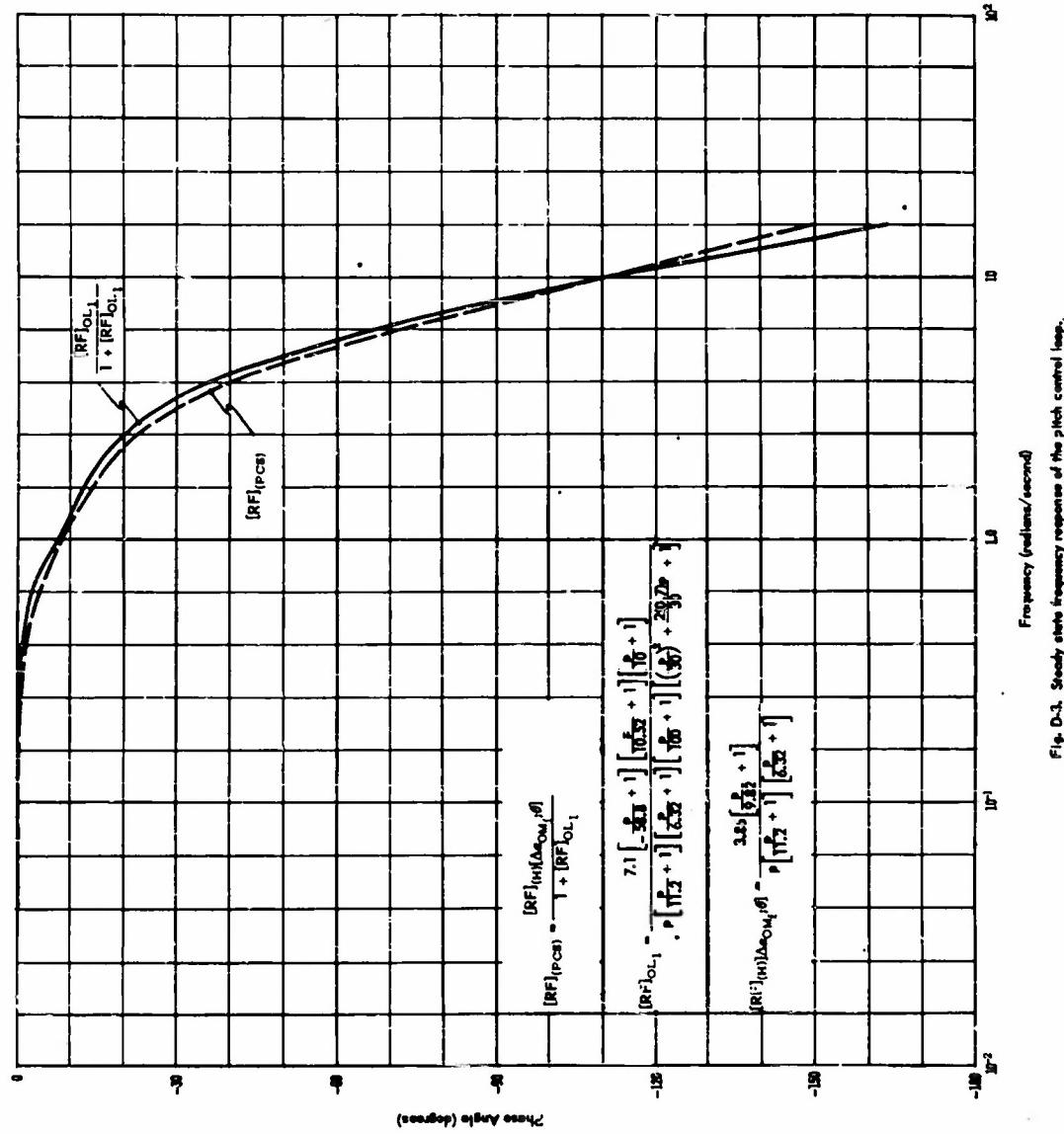
Fig. D-3. Steady state frequency response of the pitch control loop.

part of the altitude control system, a stable relating function can be derived for the altitude control system.

From Fig. (2-2), the following equations are seen to be correct.

$$\theta = \left[RF\right]_{(H)[\delta_t;\theta]} \delta_t + \left[RF\right]_{(H)[\delta_\varsigma;\theta]} \delta_f \tag{D-8}$$

$$\delta_f = \left[RF\right]_{(GU)[\theta;\varepsilon]} \left[RF\right]_{(SM)[\varepsilon;\varepsilon]} \left[RF\right]_{(FS)[\varepsilon;\delta]} \theta \tag{D-9}$$

$$h = \left[RF\right]_{(H)[\delta_t;h]} \delta_t + \left[RF\right]_{(H)[\delta_\varsigma;h]} \delta_f \tag{D-10}$$

$$\delta_t = \left[RF\right]_{(SE)[h;\varepsilon]} \left[RF\right]_{(RS)[\varepsilon;\delta]} h \tag{D-11}$$

Combining the above equations gives:

$$\left[RF\right]_{(ACS)_{OL}} = \left\{\left[RF\right]_{(RS)[\varepsilon;\delta]} \left[RF\right]_{(SE)[h;\varepsilon]}\right\} \times$$

$$\left\{\left[RF\right]_{(H)[\delta_t;h]} - \left[RF\right]_{(H)[\delta_\varsigma;h]} \left[\frac{\left[RF\right]_{(PCS)_{OL}}}{1+\left[RF\right]_{(PCS)_{OL}}}\right] \frac{\left[RF\right]_{(H)[\delta_t;\theta]}}{\left[RF\right]_{(H)[\delta_\varsigma;\theta]}}\right\} \tag{D-12}$$

From Figs. (D-2) and (D-3), the relation of the pitch control system closed loop for a foil deflection input and a pitch angle out is seen to have a magnitude of 0.72 and a phase angle of 138 degrees at a frequency of 13.1 radians per second. Thus, if one goes through the algebra, the relating

function of the altitude control loop has the point of neutral stability at $S_{(\varepsilon e)}S_{(rs)}$ equal to 0.80 with a frequency of 13.1 radians per second. These values were used as the overall system check of the computer. (See Fig. E-1).

APPENDIX E

SIMULATION OF THE HYDROFOIL CONTROL
SYSTEM ON ANALOG COMPUTER

Figure E-1 is a diagram of the simulated hydrofoil control system as used to study the steady-state system responses to sinusoidal inputs. The diagram contains four basic electronic components: the integrator, represented by a triangle changes the sign and integrates the input with a gain of ten in one-tenth real time; the summation amplifier, represented by a rectangle, amplifies each input by a factor of one, five or ten, changes the sign, and sums the result; the attenuator, represented by a square at the input to either an integrator or an amplifier, attenuates the input by a factor of five or ten; and the potentiometer, represented by the circle, attenuates the signals according to the potentiometer setting. The basic components are arranged so that the voltage response represents the response of the physical system.

The complete simulated system was excited by a combination of sinusoidal inputs representing orbital motion at the front and rear foils and sea surface at the center of gravity of the craft (refer to Appendix A). These inputs and the response of the craft were recorded on a four-channel Sanborn recorder. These quantities were measured at the points indicated on the diagram.

The equations simulated here are Eqs. (B-3) and (B-4) of Appendix B and Eqs. (D-1), (D-2), (D-3), (D-6), and (D-7) of Appendix D. Equation (B-4) is broken down into X and Z forces, and the moments are calculated by the computer. Constant coefficients are assumed for these equations so that potentiometers can be used rather than active networks. The potentiometer coefficient settings for the above equations are:
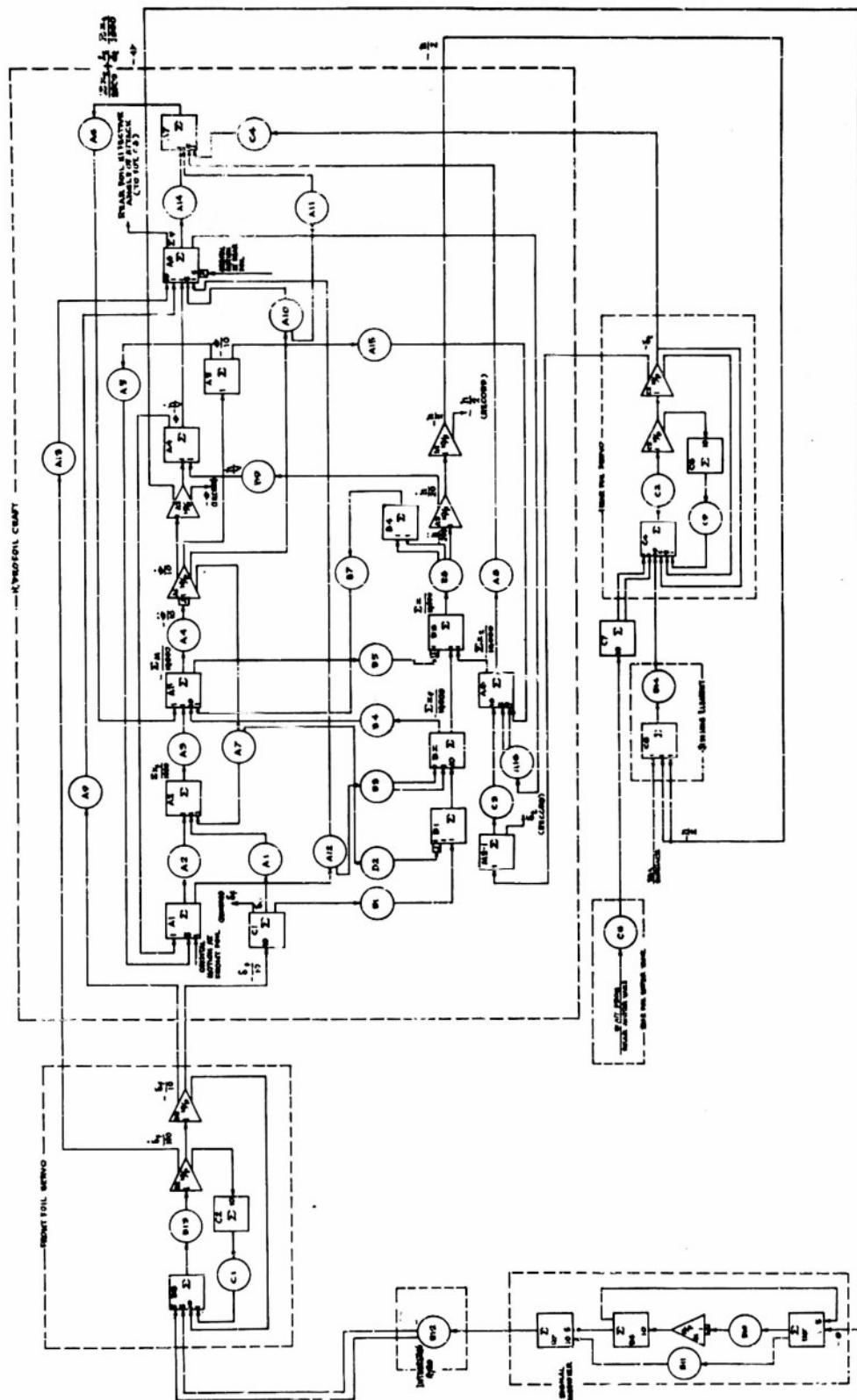
FIG. E - 1   WIRING DIAGRAM OF HYDROFOIL CONTROL SYSTEM ON ANALOG COMPUTER

$$A1 = 0.503 = \frac{\left(\frac{\partial C_D}{\partial \alpha}\right)_f S_f q}{1000}$$

$$A2 = 0.395 = \frac{\left(C_L - \frac{\partial C_D}{\partial \alpha}\right)_f S q}{1000}$$

$$A3 = 0.375 = \frac{d_f}{10}$$

$$A4 = 0.307 = \frac{1000}{I_y - M_{\ddot{\theta}}}$$

$$A5 = 0.375 = \frac{2 l_f}{V}$$

$$A6 = 0.750 = \frac{d_t}{5}$$

$$A7 = 0.257 = \frac{C_{Df} S_f \rho V d_f}{100}$$

$$A8 = 0.640 = \frac{l_t}{d_t}$$

$$A9 = 0.890 = 10 \frac{\partial \epsilon}{\partial \alpha}$$

$$A10 = 0.207 = \frac{2\left(l_t + l \frac{\partial \epsilon}{\partial \alpha}\right)}{V}$$

$$A11 = 0.292 = \frac{C_{Dt} S_t \rho V d_t}{200}$$

$$A12 = 0.089 = \frac{\partial \epsilon}{\partial \alpha}$$

$$A13 = 0.237 = \frac{10l}{V}\frac{\partial \epsilon}{\partial \alpha}$$

$$A14 = 0.519 = \frac{RS_t q}{2000}$$

$$A15 = 0.523 = \frac{C_{Lt} S_t \rho V d_t}{1000}$$

$$A16 = 0.310 = \frac{NS_t q}{100,000}$$

$$B1 = 0.140 = \frac{\left(\frac{\partial C_L}{\partial \alpha}\right)_f S_f q}{100,000}$$

$$B2 = 0.230 = \frac{C_{Lf} S_f \rho V d_f}{1000}$$

$$B3 = 0.700 = \frac{5\left[\frac{\partial C_L}{\partial \alpha} + C_D\right]_f S_f q}{100,000}$$

$$B4 = 0.560 = \frac{l_f}{10}$$

$$B5 = 0.043 = \frac{10 Z_{\ddot{\theta}}}{I_y - M_{\ddot{\theta}}}$$

$$B6 = 0.383 = \frac{50}{m + Z_{\ddot{h}}}$$

$$B7 = 0.550 = \frac{M_{\ddot{h}}}{100}$$

$$B9 = 0.660 = \frac{20}{V}$$

66

$$B_{10} = 1.000 = \frac{i}{100\,\tau_{sm}}$$

$$B_{11} = 1.000 = \frac{\alpha_{sm}}{10}$$

$$B_{12} = \text{variable} = \frac{S_{sm}\,S_g\,S_{FS}}{10}$$

$$B_{13} = 0.900 = \frac{\omega_{FS}^2}{1000}$$

$$B_{14} = \text{variable} = S_{RS}\,S_{SE}$$

$$C_1 = 0.487 = \frac{20\,\zeta_{FS}}{\omega_{FS}}$$

$$C_2 = 0.900 = \frac{\omega_{RS}^2}{1000}$$

$$C_3 = 0.317 = \frac{\left(\frac{\partial C_L}{\partial \alpha}\right)_t S_t\,q}{100,000}$$

$$C_4 = 0.483 = \frac{\left(\frac{\partial C_D}{\partial \alpha}\right)_t S_t\,q}{2000}$$

$$C_6 = \text{variable} = \frac{S_{RS}\,S_{RWV}}{2}$$

$$C_9 = 0.467 = \frac{20\,\zeta_{RS}}{\omega_{RS}}$$

APPENDIX F

BIBLIOGRAPHY

1. St. Denis and Pierson, "On the Motions of Ships in Confused Seas", paper for Society of Naval Architects and Marine Engineers, Nov. 1953.

2. Buermann, Leehey, and Stilwell, "An Appraisal of Hydrofoil Supported Craft", paper for Society of Naval Architects and Marine Engineers, November 1953.

3. Amster, "Hydrofoil Studies and Preliminary Design Data", report of Joshua Hendy Corporation, 612 South Flower Street, Los Angeles 17, Calif., June 30, 1950.

4. Wedan, "Preliminary Analysis of Height-Controlled Hydrofoil Systems with Fully Submerged Foils", report of Flight Control Laboratory, Mass. Inst. of Tech., Cambridge, Mass. Sept. 1953.

5. Connors, report SAG-M-1 of Flight Control Laboratory, Mass. Inst. of Tech., Cambridge, Mass., 1954.

6. Wellinger, report SAG-M-2, same as Ref. (5).

7. Wellinger, report SAG-W-1, same as Ref. (5).

8. Wellinger, report SAG-W-2, same as Ref. (5).

9. Barnes, report SAG-W-3, same as Ref. (5).

10. Wellinger report SAG-W-4, same as Ref. (5).

11. Wellinger, report SAG-W-5, same as Ref. (5).

12. Lemon and Ference, "Analytical Experimental Physics", University of Chicago Press Chicago 37, Ill. Revised 1946.

13. Cronk and Jones, "Time Lags in Force Buildup on Hydrofoils", Memorandum Report of Fluidyne Engineering Corporation, July 1953.

14. Whitman, Wales and Andersen, "The Type H Gyro, Computing and Accelerometer Units", Report R-17 of the Instrumentation Laboratory, Mass. Inst. of Tech., Cambridge Mass., Sept. 1953, (declassified from Confidential).

15. Seamans, Barnes, Garber and Howard "Recent Developments in Aircraft Control", paper for the Institute of Aeronautical Sciences, January 1954.

16. Draper, McKay and Lees, "Instrument Engineering", Volumes I and II, McGraw-Hill Book Company, New York, 1952.